

Bacterial Cell Death to Overcome Drug Resistance with Multitargeting Bis-Naphthalimides as Potent Antibacterial Agents Against *Enterococcus faecalis*

Saurabh Gupta, Vijay Luxami, Kamaldeep Paul*

Department of Chemistry and Biochemistry, Thapar Institute of Engineering and Technology,
Patiala-147001, India

*Email: kpaul@thapar.edu

Table of Contents

	Contents	Page No
Figures S1-S34	¹ H and ¹³ C NMR of compounds	3
	Biological assays procedures	20
	Antibacterial assays	20
	Minimal Bactericidal Concentrations (MBC) assays	20
	Bacterial susceptibility evaluation	20-21
	Drug Combination	21
Table S1	Combination effect of 5d and 5o with tetracycline and amoxicillin against <i>B. subtilis</i>	21
Table S2	Combination effect of 5d and 5o with tetracycline and amoxicillin against <i>L. species</i>	21
Table S3	Combination effect of 5d and 5o with tetracycline and amoxicillin against <i>S. aureus</i>	21
Table S4	Combination effect of 5d and 5o with tetracycline and amoxicillin against <i>E. coli</i>	21-22
Table S5	Combination effect of 5d and 5o with tetracycline and amoxicillin against <i>S. enterica</i>	22
Table S6	Combination effect of 5d and 5o with tetracycline and amoxicillin against <i>A. calcoaceticus</i>	22
Table S7	Combination effect of 5d and 5o with tetracycline and amoxicillin against <i>S. marcescens</i>	22
	Time-killing kinetics of <i>Enterococcus faecalis</i>	23
	Cytotoxicity toward cancer cell lines	23
	Cytotoxicity toward normal cell line	23
Table S8	Cytotoxicity of derivatives 5a-5h at 10 μM concentration	23-24
Table S9	Cytotoxicity of derivatives 5i-8p at 10 μM concentration.	25-26
	Anti-biofilm Assay	26
	Outer membrane disruption	26
	Inner membrane disruption	26-27
	Leakage of intercellular protein	27
	Metabolic activity	27
	Scanning Electron Microscopy (SEM)	27
	Reactive Oxygen Species (ROS) production	27-28
	Intracellular glutathione activity	28
	Lipid peroxidation	28
Hemolysis Assay	28-29	

Figure S35	Fluorescence spectra of ethidium bromide and ct-DNA complexes upon gradual addition of compounds (a) 5d and (b) 5o	29
Table S10	Docked pose of compounds 5a – 5p	29-34
Table S11	Molecular docking of compounds 5d and 5o	34-35
Table S12	Molecular docking of compounds 5a - 5h	35
Table S13	Molecular docking of compounds 5i - 5p	35-36
Figure S36	Benesi-Hildebrand plots of compounds 5d and 5o	36
Table S14	Binding parameters for compounds 5d and 5o at three different temperatures	36
Table S15	Thermodynamic parameters of HSA binding with compounds 5d and 5o	36
Figure S37	Stern-Volmer plots of HSA with compounds 5d and 5o	37
Figure S38	Modified Stern-Volmer plots of HSA with compounds 5d and 5o	37
Figure S39	Time decay profile of HSA on progressive addition of compounds	37
Table S16	Lifetime fluorescence decay of HSA on interaction with 5d and 5o	37-38
Figure S40	Fluorescence spectra of bare HSA (blue) in the presence of compounds and in the presence of SDS.	38
Table S17	Atomic orbital HOMO-LUMO composition of compounds 5a – 5p	38-40
	Sample preparation	40
	UV-Vis absorption spectroscopy	40-41
	Fluorescence emission spectroscopy	41
	Competitive displacement assay	41
	Docking simulation	41-42
	References	42

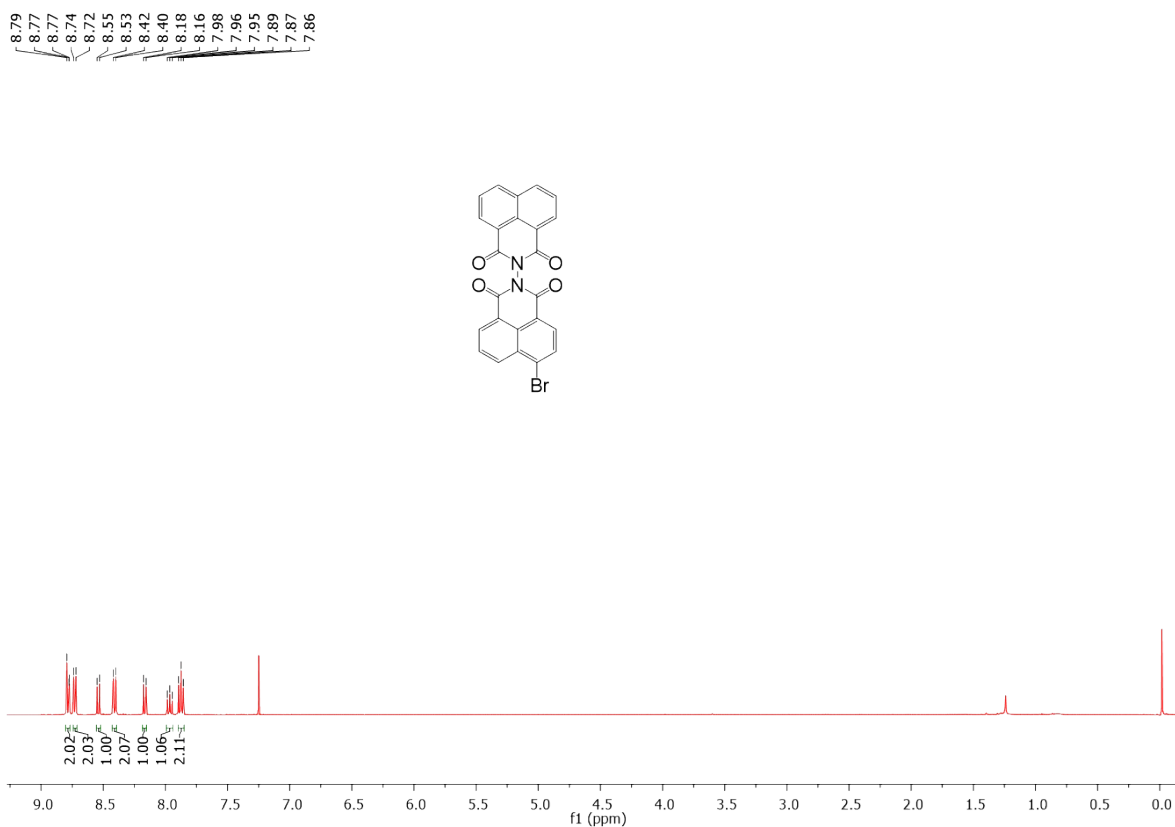


Figure S1. ¹H NMR spectrum of 6-bromo-1*H*,1'*H*,3*H*,3'*H*-[2,2'-bibenzo[*de*]isoquinoline]-1,1',3,3'-tetraone (**4**)

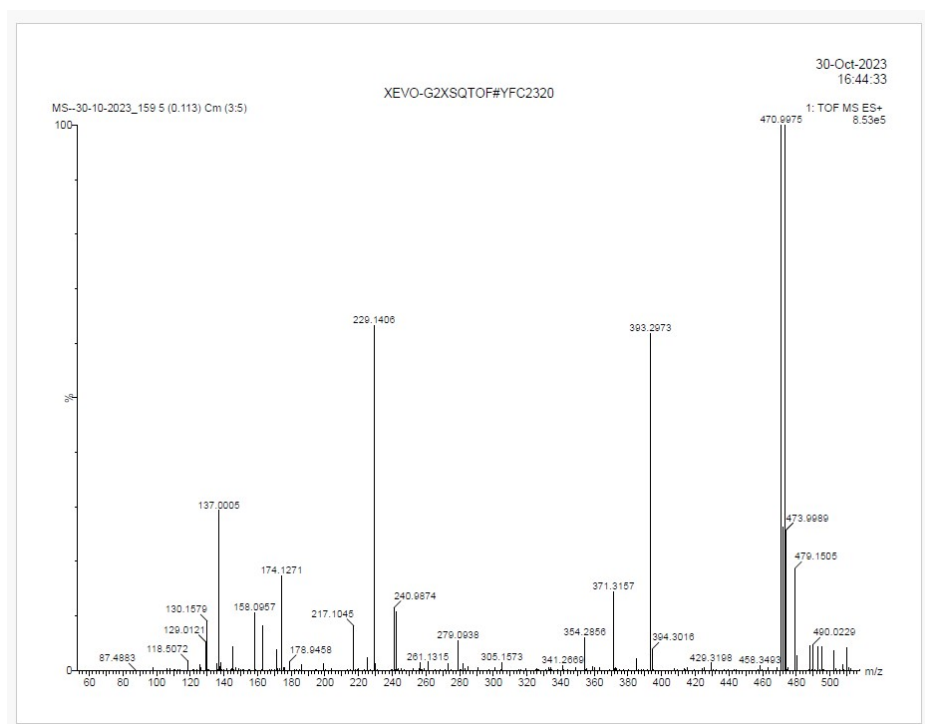


Figure S2: HRMS of 6-bromo-1*H*,1'*H*,3*H*,3'*H*-[2,2'-bibenzo[*de*]isoquinoline]-1,1',3,3'-tetraone (**4**)

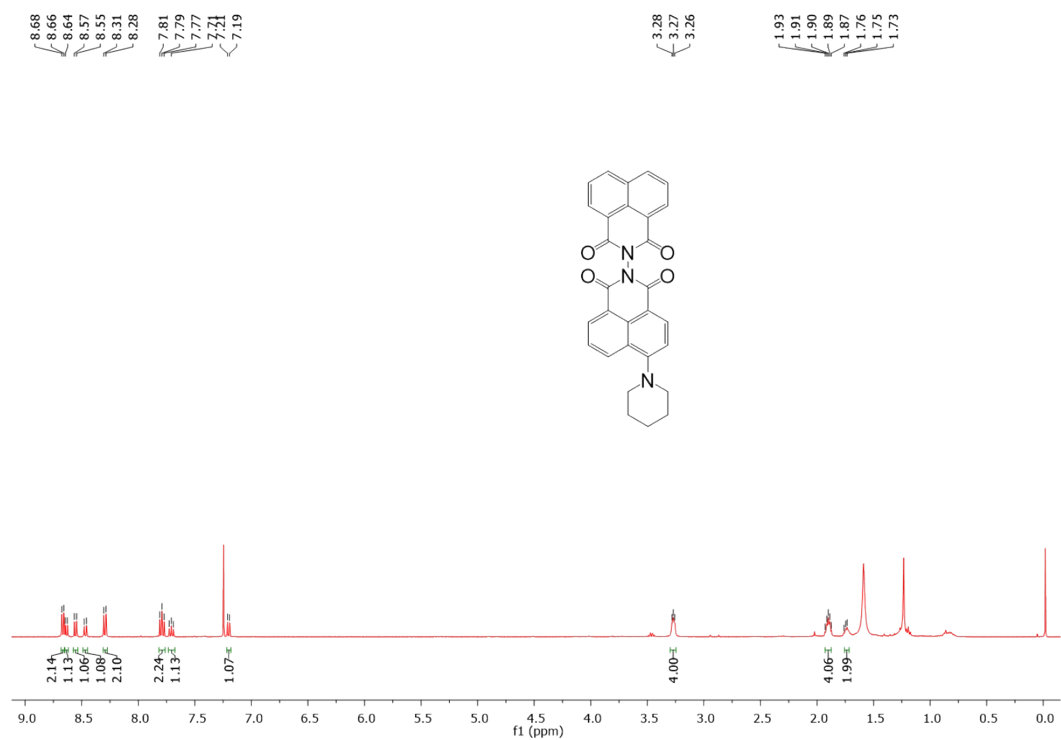


Figure S3. ¹H NMR spectrum of 6-(piperidin-1-yl)-1*H*,1'*H*,3*H*,3'*H*-[2,2' bibenzo[*de*]isoquinoline]-1,1',3,3'-tetraone (**5a**)

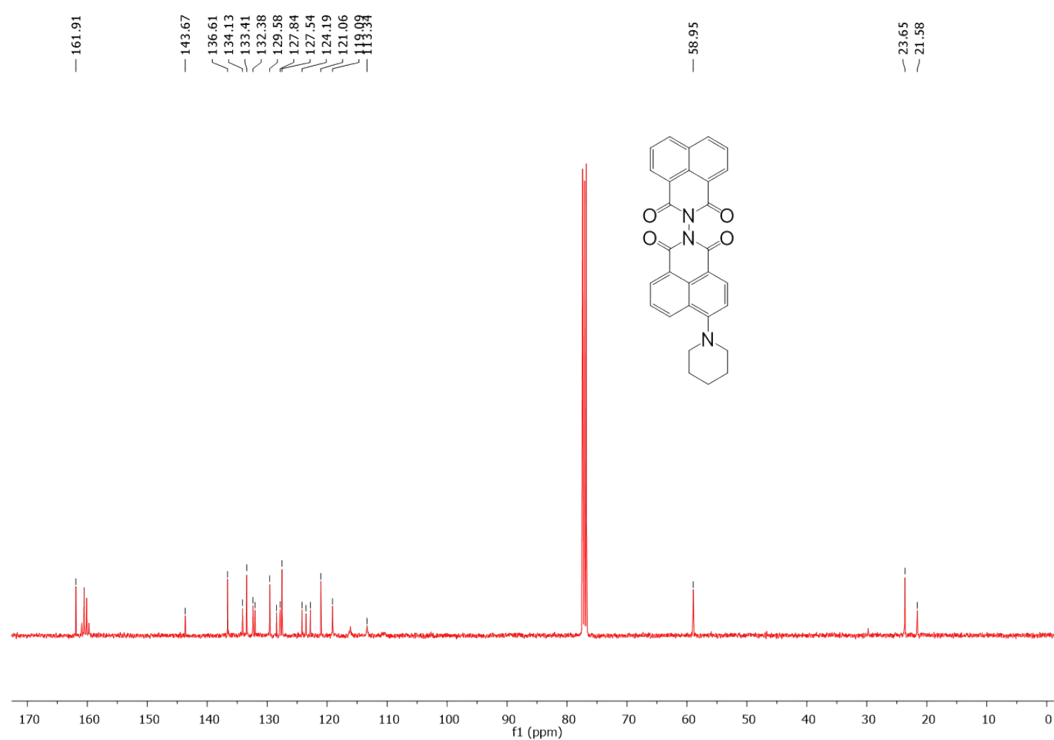


Figure S4. ¹³C NMR spectrum of 6-(piperidin-1-yl)-1*H*,1'*H*,3*H*,3'*H*-[2,2' bibenzo[*de*]isoquinoline]-1,1',3,3'-tetraone (**5a**)

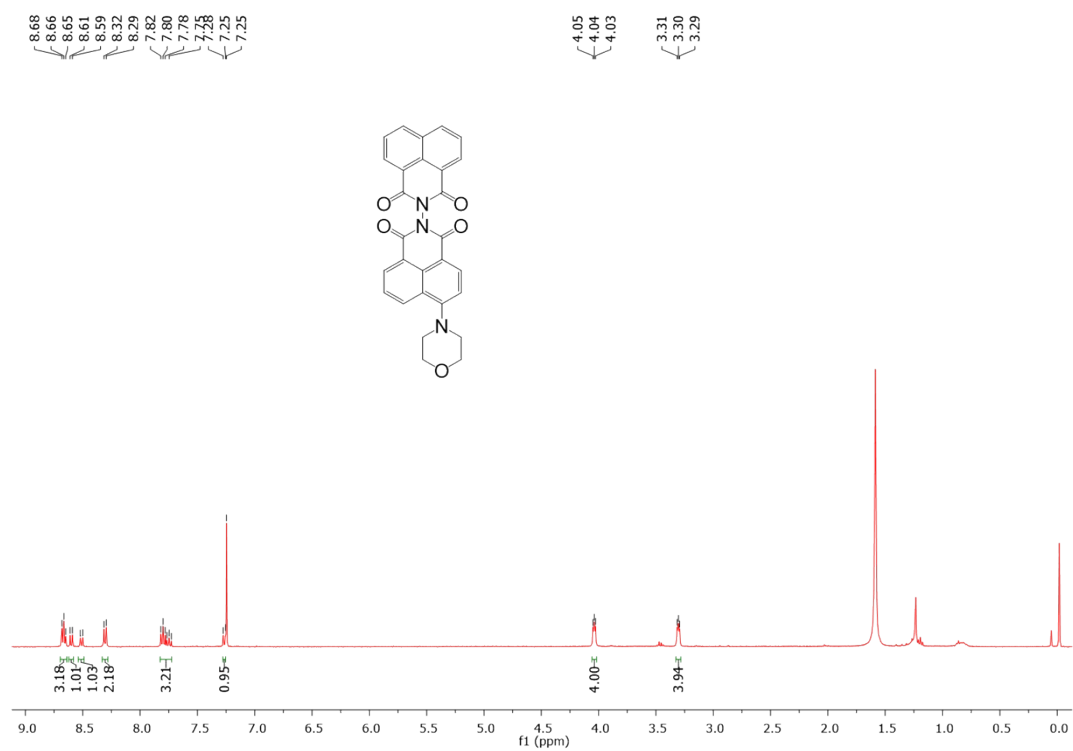


Figure S5. ¹H NMR spectrum of 6-morpholino-1H,1'H,3H,3'H-[2,2'-bibenzo[de]isoquinoline]-1,1',3,3'-tetraone (**5b**)

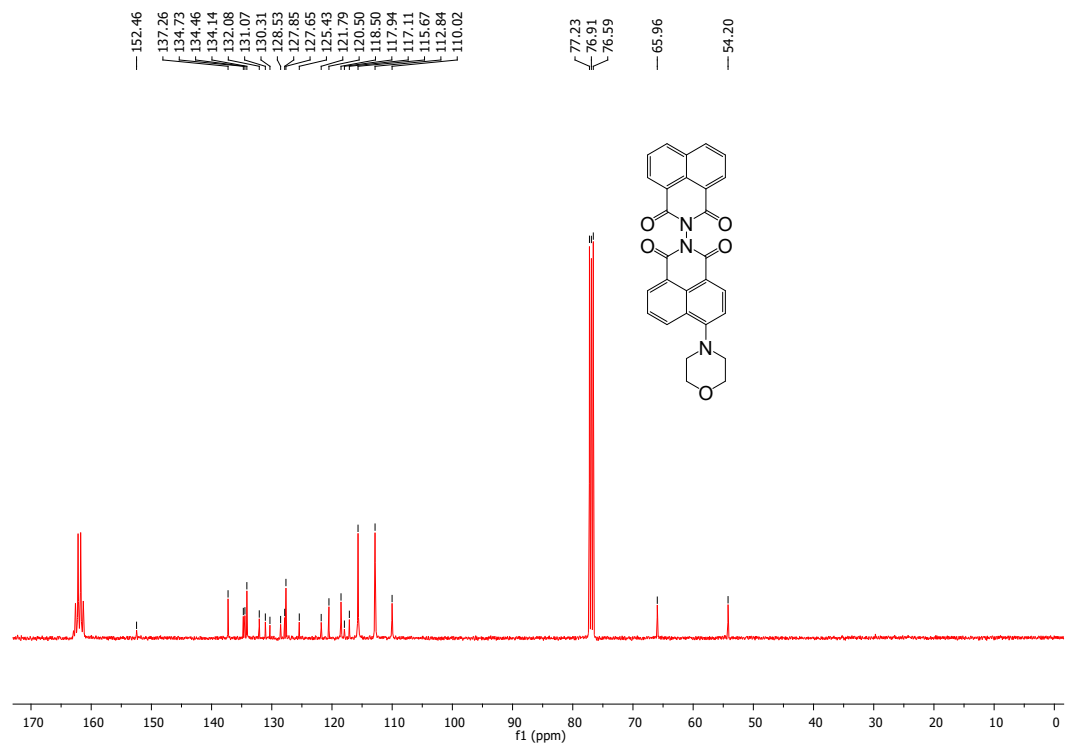


Figure S6. ^{13}C NMR spectrum of 6-morpholino-1*H*,1'*H*,3*H*,3'*H*-[2,2'-bibenzo[*de*]isoquinoline]-1,1',3,3'-tetraone (**5b**)

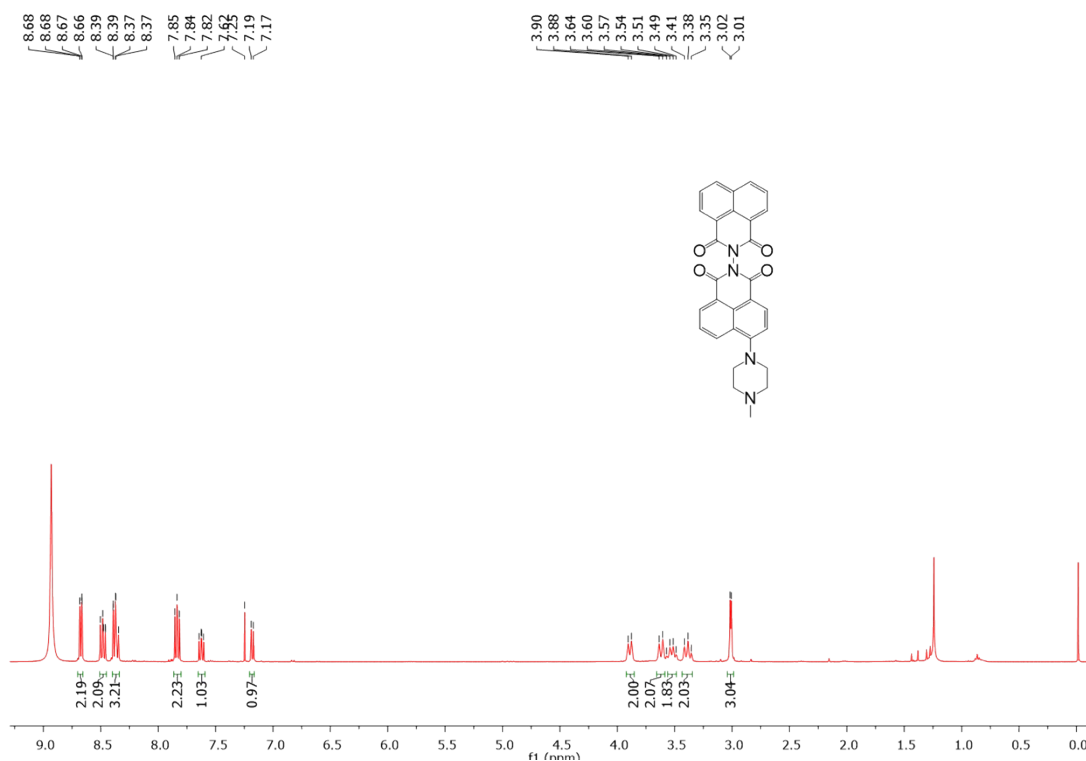


Figure S7. ^1H NMR spectrum of 6-(4-methylpiperazin-1-yl)-1*H*,1'*H*,3*H*,3'*H*-[2,2'-bibenzo[*de*]isoquinoline]-1,1',3,3'-tetraone (**5c**)

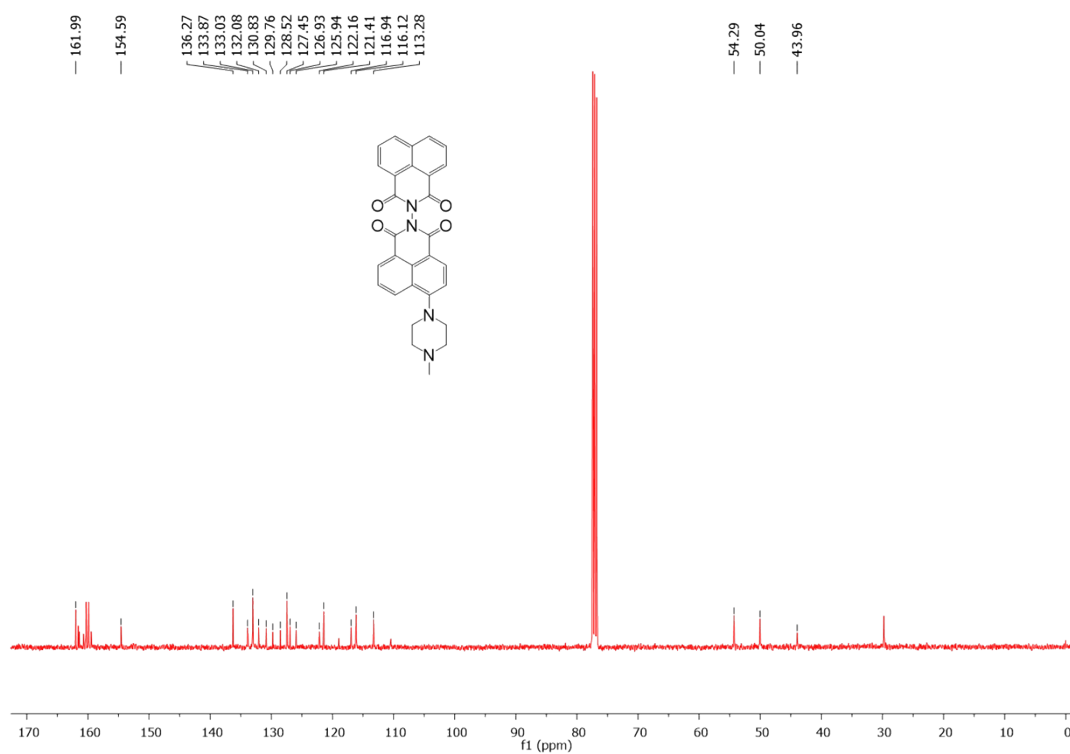


Figure S8. ^{13}C NMR spectrum of 6-(4-methylpiperazin-1-yl)-1*H*,1'*H*,3*H*,3'*H*-[2,2'-bibenzo[*de*]isoquinoline]-1,1',3,3'-tetraone (**5c**)

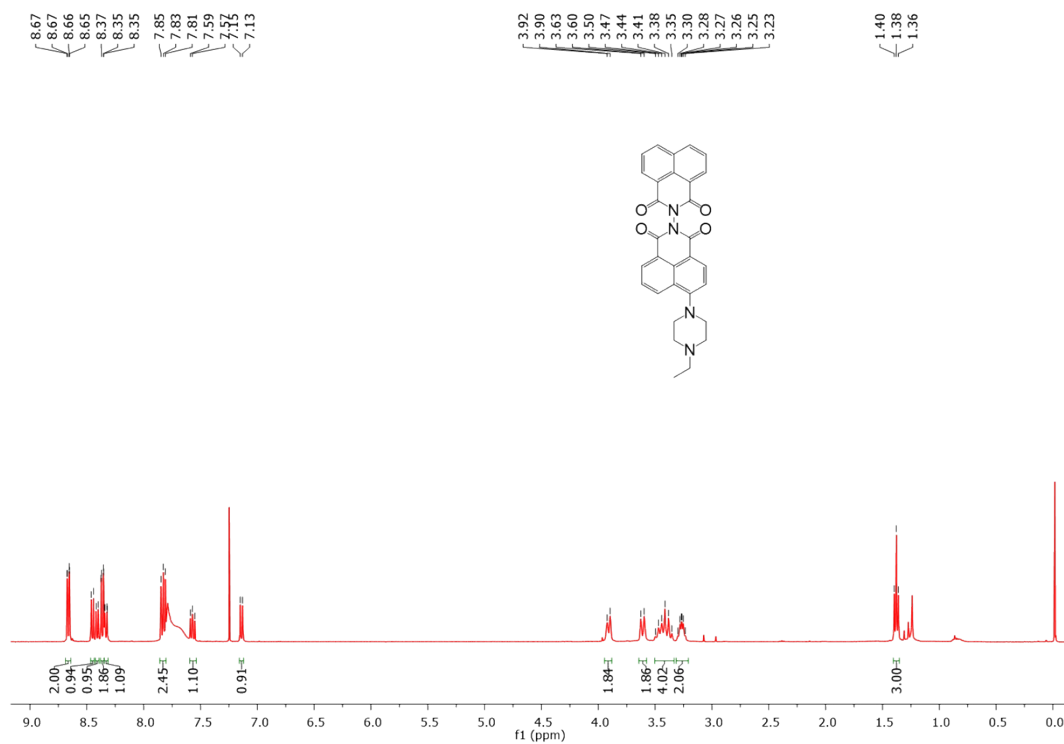


Figure S9. ^1H NMR spectrum of 6-(4-ethylpiperazin-1-yl)-1*H*,1'*H*,3*H*,3'*H*-[2,2'-bibenzo[*de*]isoquinoline]-1,1',3,3'-tetraone (**5d**)

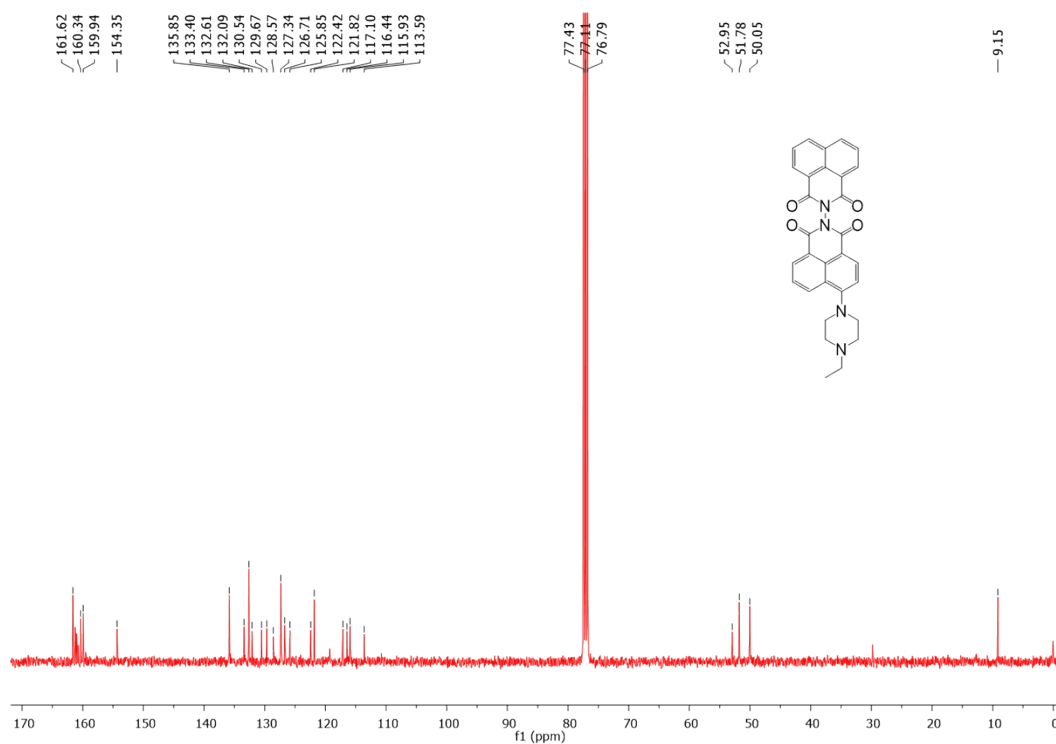


Figure S10. ^{13}C NMR spectrum of 6-(4-ethylpiperazin-1-yl)-1*H*,1'*H*,3*H*,3'*H*-[2,2'-bibenzo[de]isoquinoline]-1,1',3,3'-tetraone (**5d**)

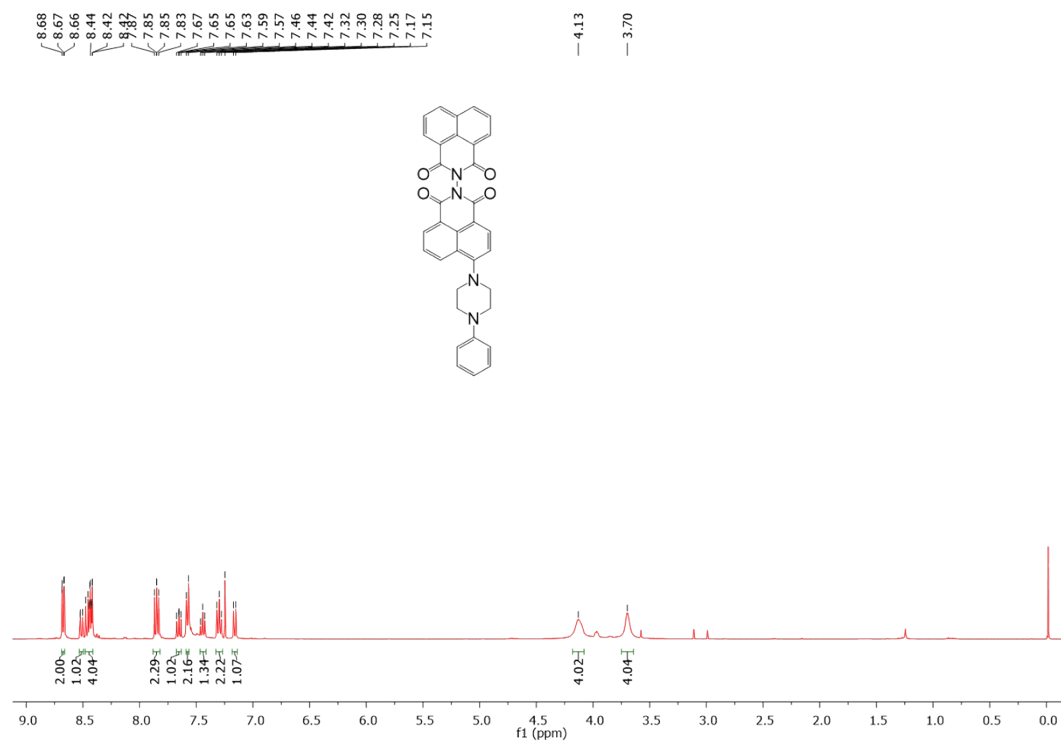


Figure S11. ^1H NMR spectrum of 6-(4-phenylpiperazin-1-yl)-1*H*,1'*H*,3*H*,3'*H*-[2,2'-bibenzo[de]isoquinoline]-1,1',3,3'-tetraone (**5e**)

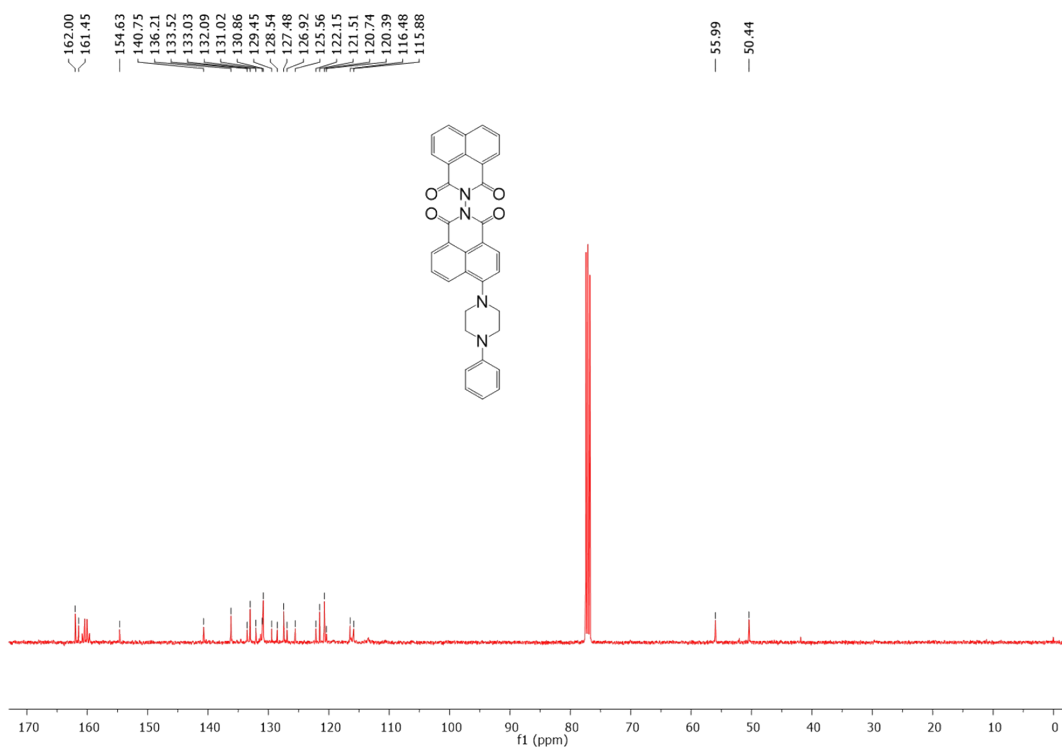


Figure S12. ^{13}C NMR spectrum of 6-(4-phenylpiperazin-1-yl)-1*H*,1'*H*,3*H*,3'*H*-[2,2'-bibenzo[*de*]isoquinoline]-1,1',3,3'-tetraone (**5e**)

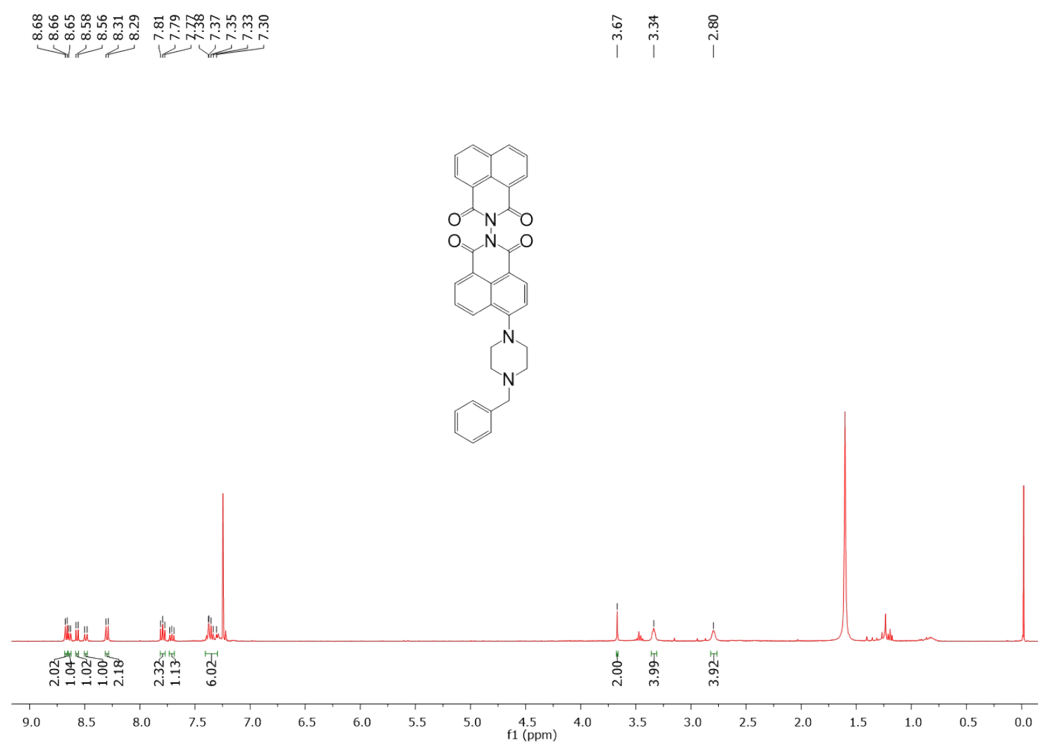


Figure S13. ^1H NMR spectrum of 6-(4-benzylpiperazin-1-yl)-1*H*,1'*H*,3*H*,3'*H*-[2,2'-bibenzo[*de*]isoquinoline]-1,1',3,3'-tetraone (**5f**)

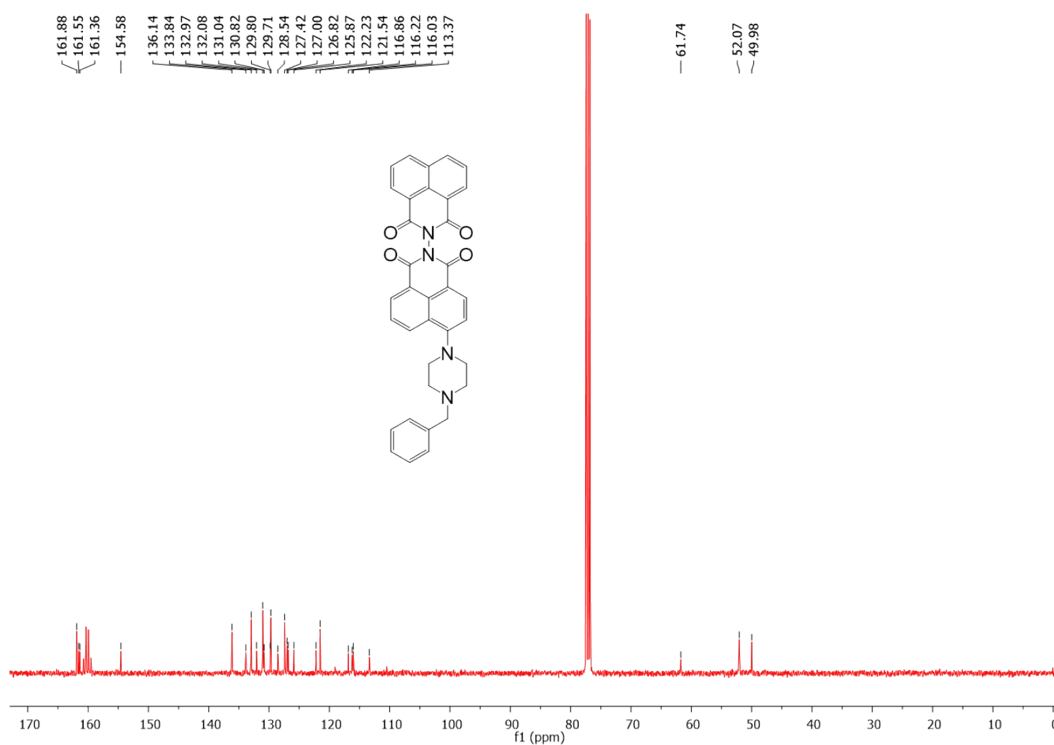


Figure S14. ^{13}C NMR spectrum of 6-(4-benzylpiperazin-1-yl)-1*H*,1'*H*,3*H*,3'*H*-[2,2'-bibenzo[*de*]isoquinoline]-1,1',3,3'-tetraone (**5f**)

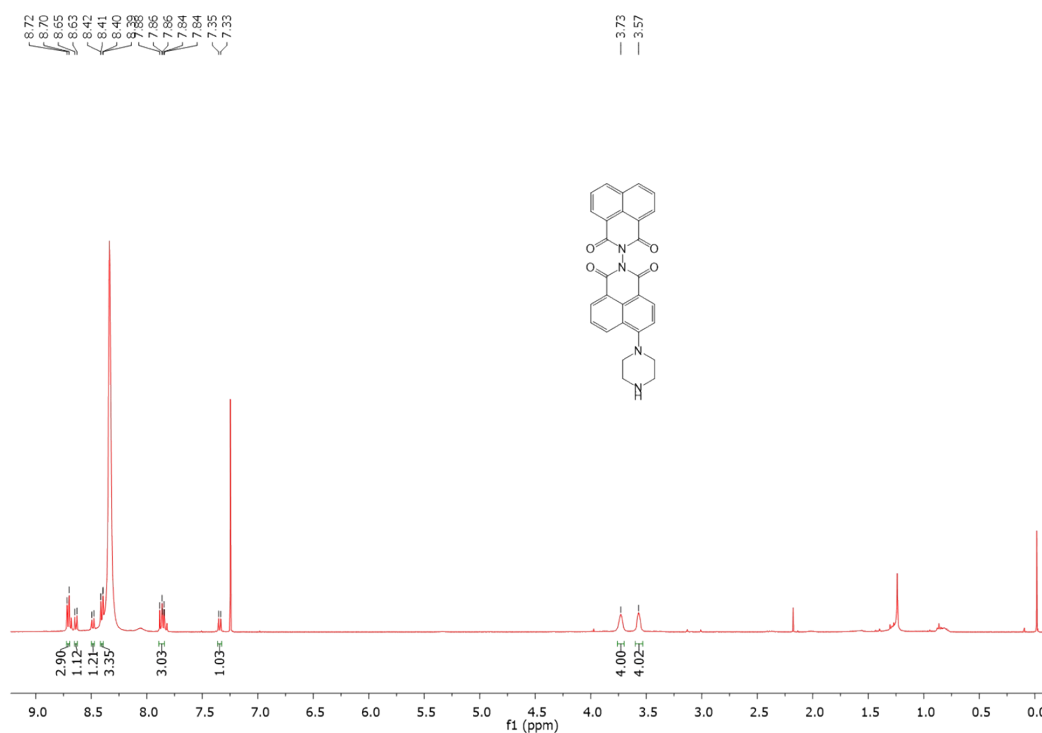


Figure S15. ^1H NMR spectrum of 6-(piperazin-1-yl)-1*H*,1'*H*,3*H*,3'*H*-[2,2'-bibenzo[*de*]isoquinoline]-1,1',3,3'-tetraone (**5g**)

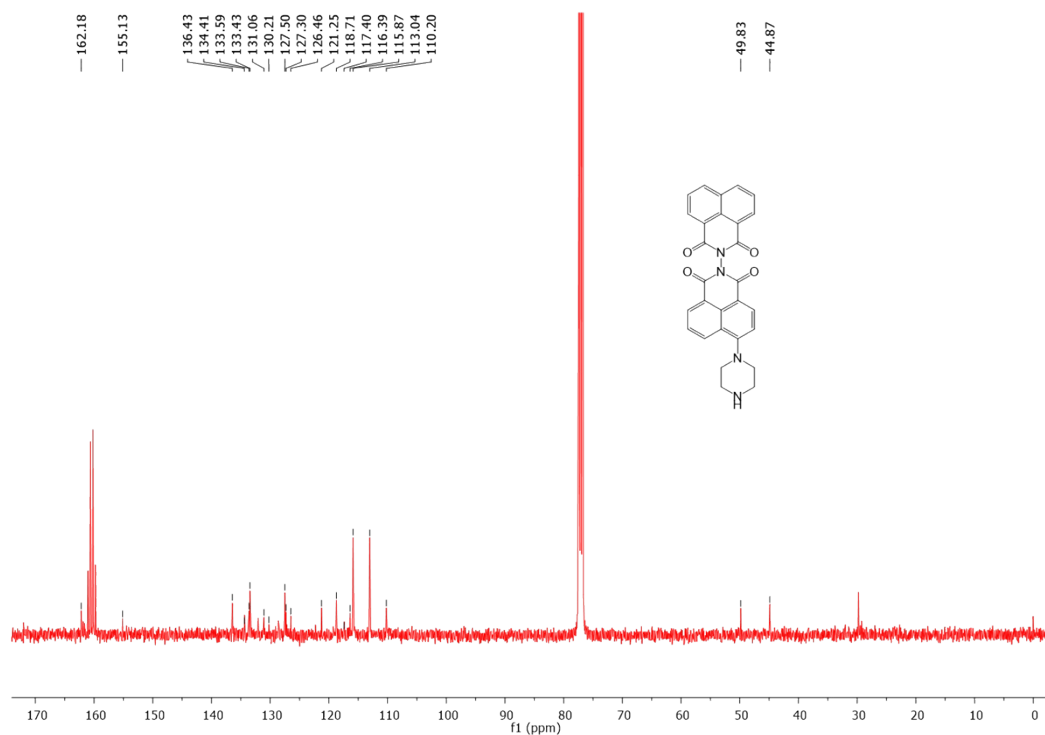


Figure S16. ^{13}C NMR spectrum of 6-(piperazin-1-yl)-1*H*,1'*H*,3*H*,3'*H*-[2,2'-bibenzo[*de*]isoquinoline]-1,1',3,3'-tetraone (**5g**)

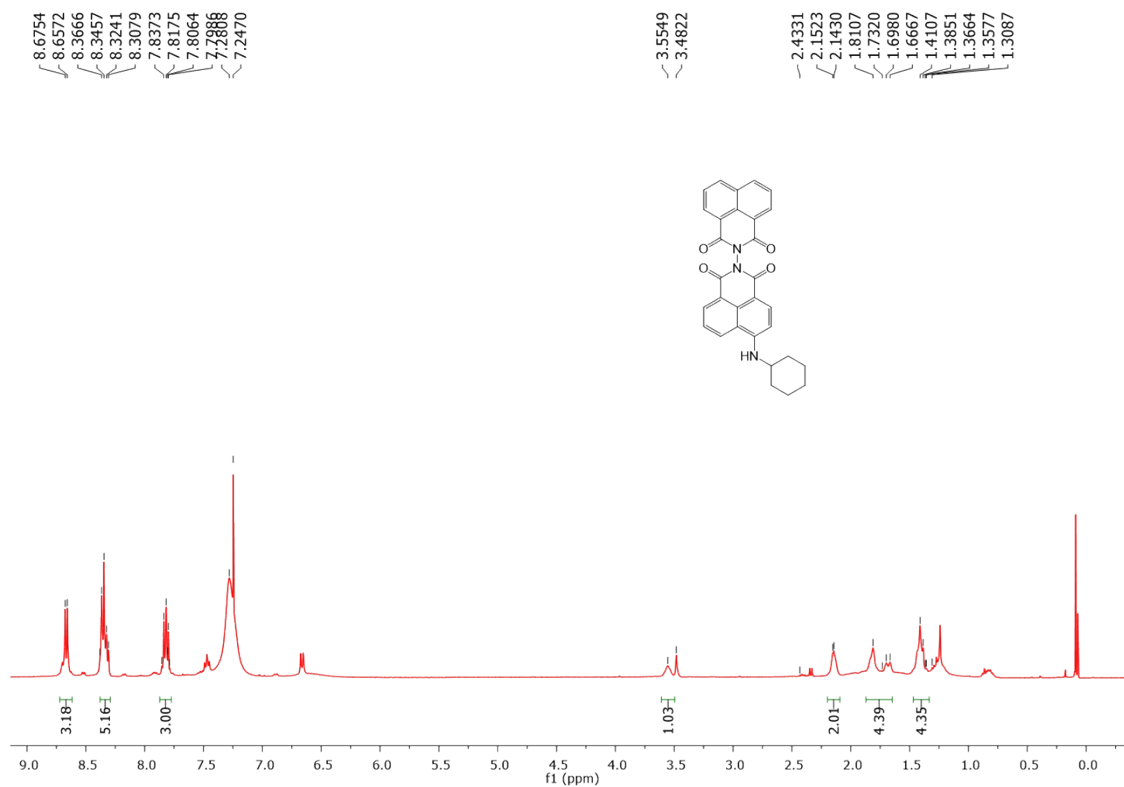


Figure S17. ^1H NMR spectrum of 6-(cyclohexylamino)-1*H*,1'*H*,3*H*,3'*H*-[2,2'-bibenzo[*de*]isoquinoline]-1,1',3,3'-tetraone (**5h**)

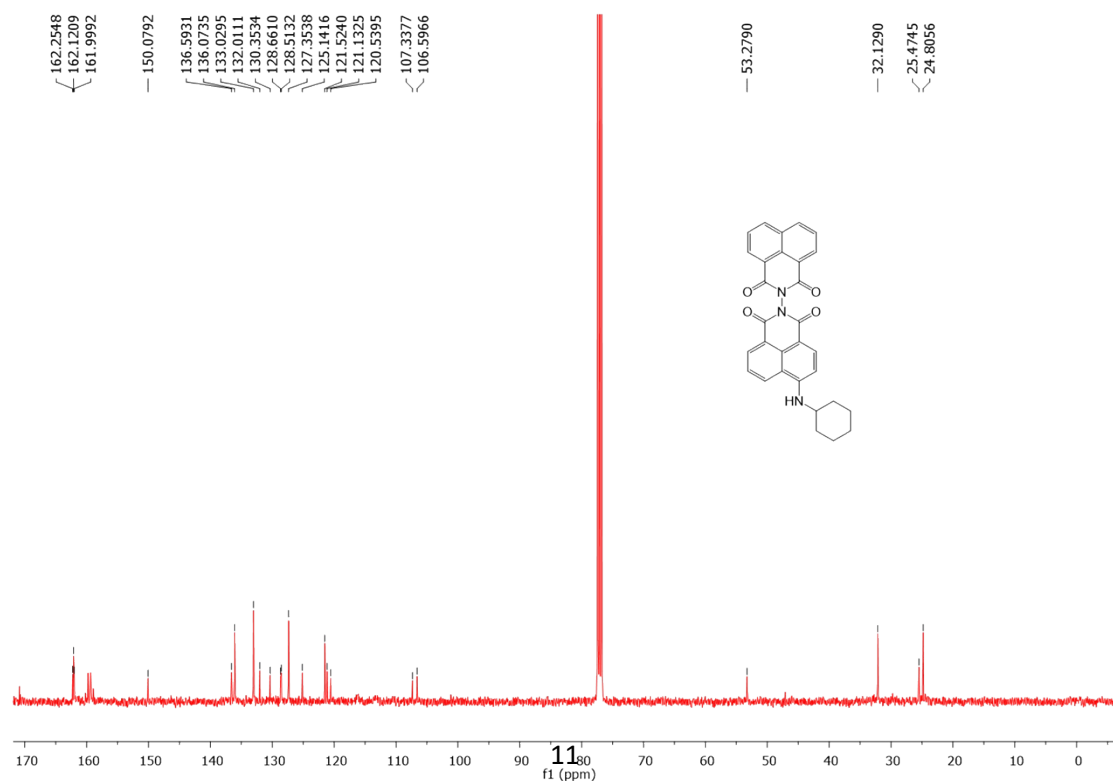


Figure S18. ^{13}C NMR spectrum of 6-(cyclohexylamino)-1*H*,1'*H*,3*H*,3'*H*-[2,2'-bibenzo[de]isoquinoline]-1,1',3,3'-tetraone (**5h**)

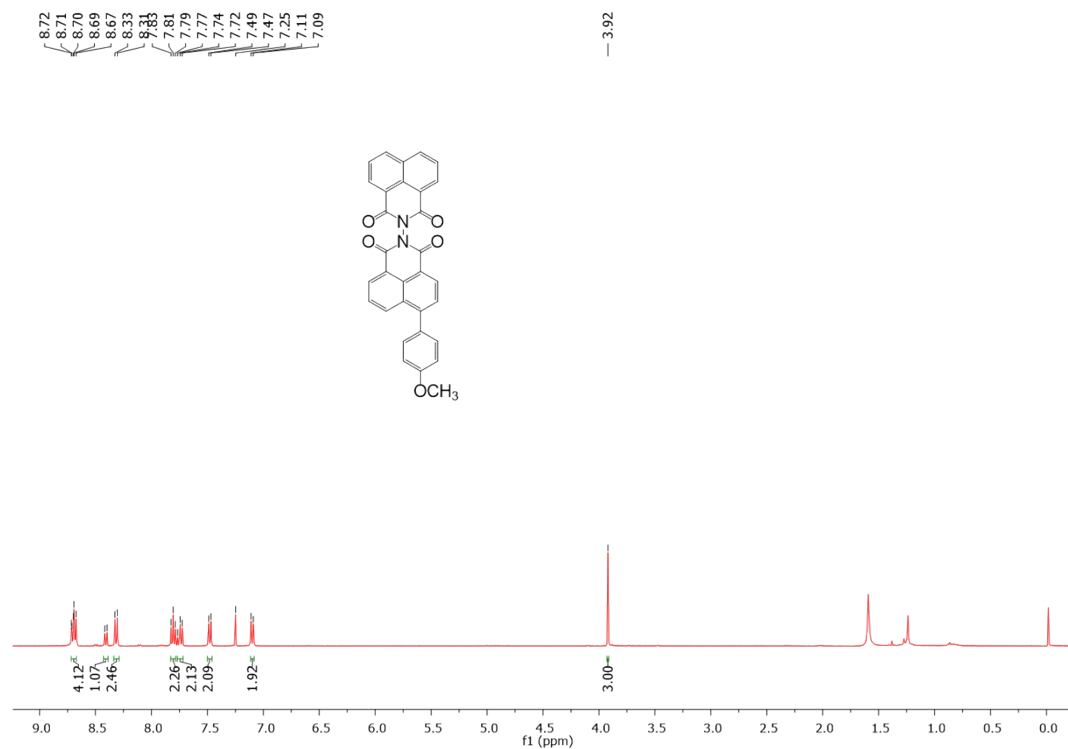


Figure S19. ^1H NMR spectrum of 6-(4-methoxyphenyl)-1*H*,1'*H*,3*H*,3'*H*-[2,2'-bibenzo[de]isoquinoline]-1,1',3,3'-tetraone (**5i**)

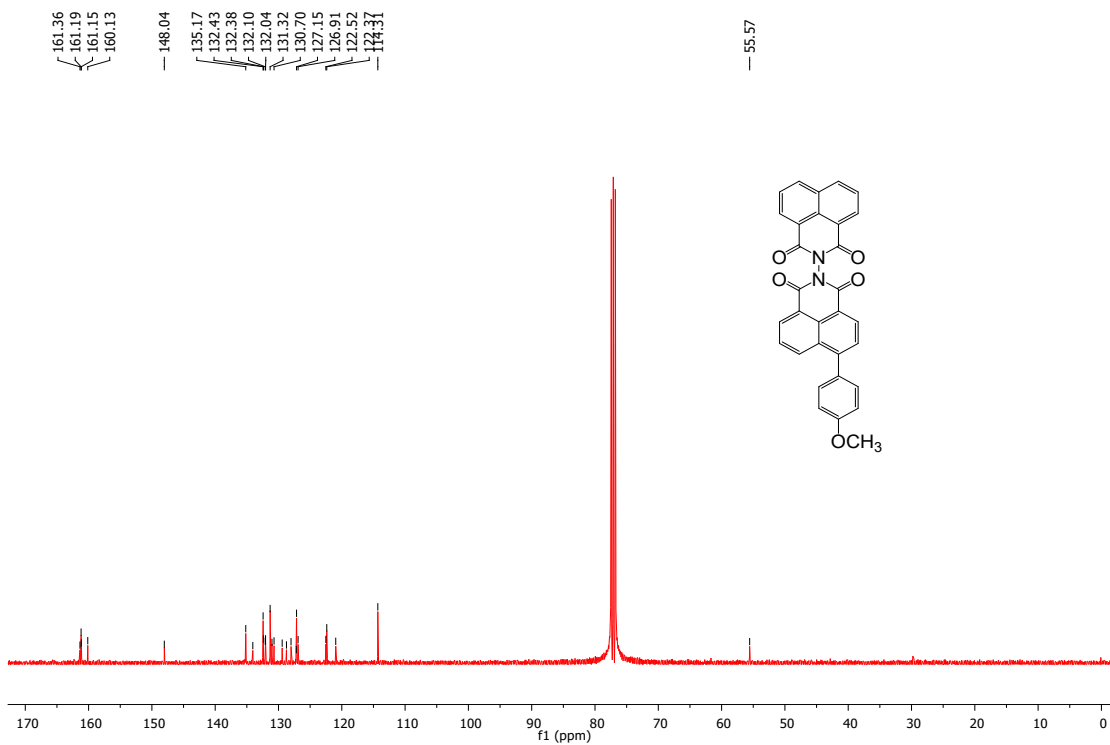


Figure S20. ^{13}C NMR spectrum of 6-(4-methoxyphenyl)-1*H*,1'*H*,3*H*,3'*H*-[2,2'-bibenzo[*de*]isoquinoline]-1,1',3,3'-tetraone (**5i**)

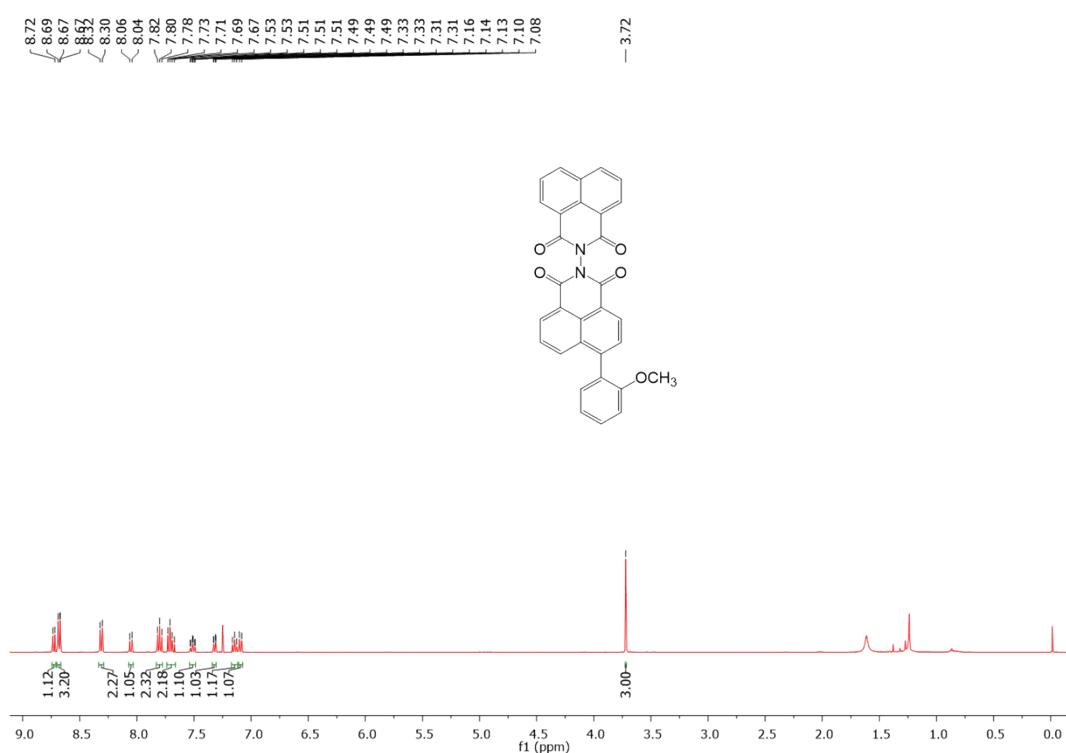


Figure S21. ^{13}C NMR spectrum of 6-(2-methoxyphenyl)-1*H*,1'*H*,3*H*,3'*H*-[2,2'-bibenzo[*de*]isoquinoline]-1,1',3,3'-tetraone (**5j**)

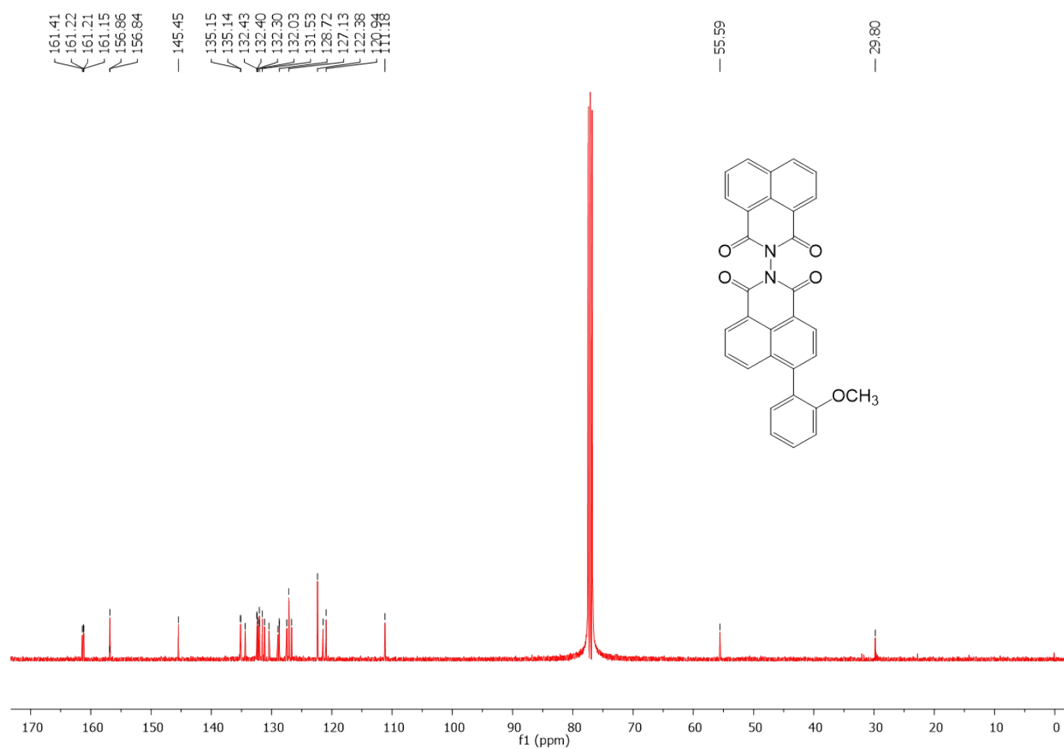


Figure S22. ¹³C NMR spectrum of 6-(2-methoxyphenyl)-1H,1'H,3H,3'H-[2,2'-bibenzo[de]isoquinoline]-1,1',3,3'-tetraone (**5j**)

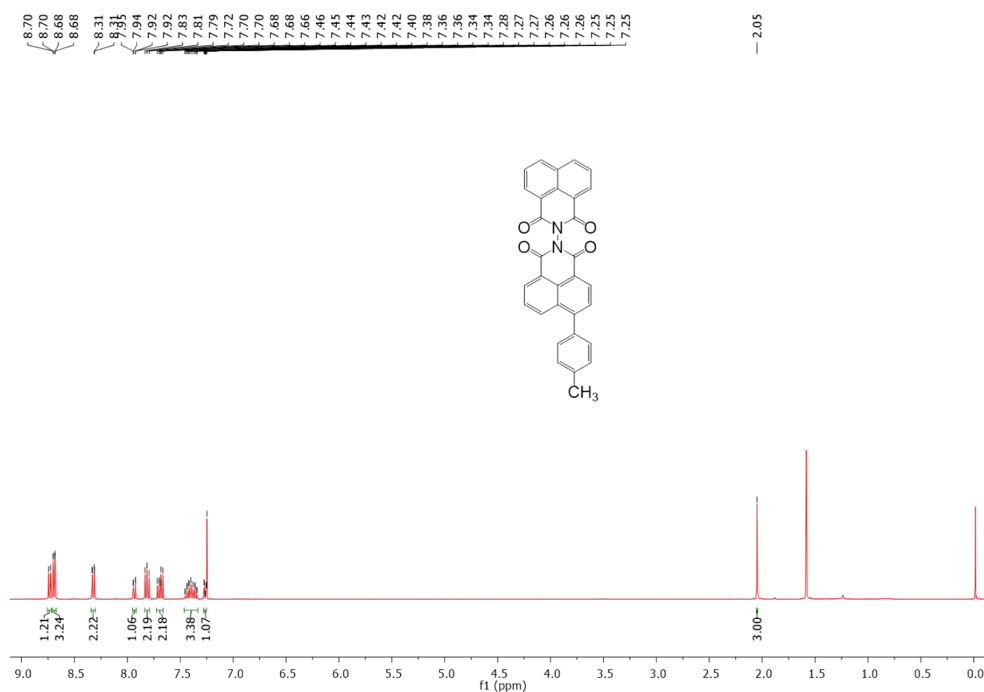


Figure S23. ¹H NMR spectrum of 6-(p-tolyl)-1H,1'H,3H,3'H-[2,2'-bibenzo[de]isoquinoline]-1,1',3,3'-tetraone (**5k**)

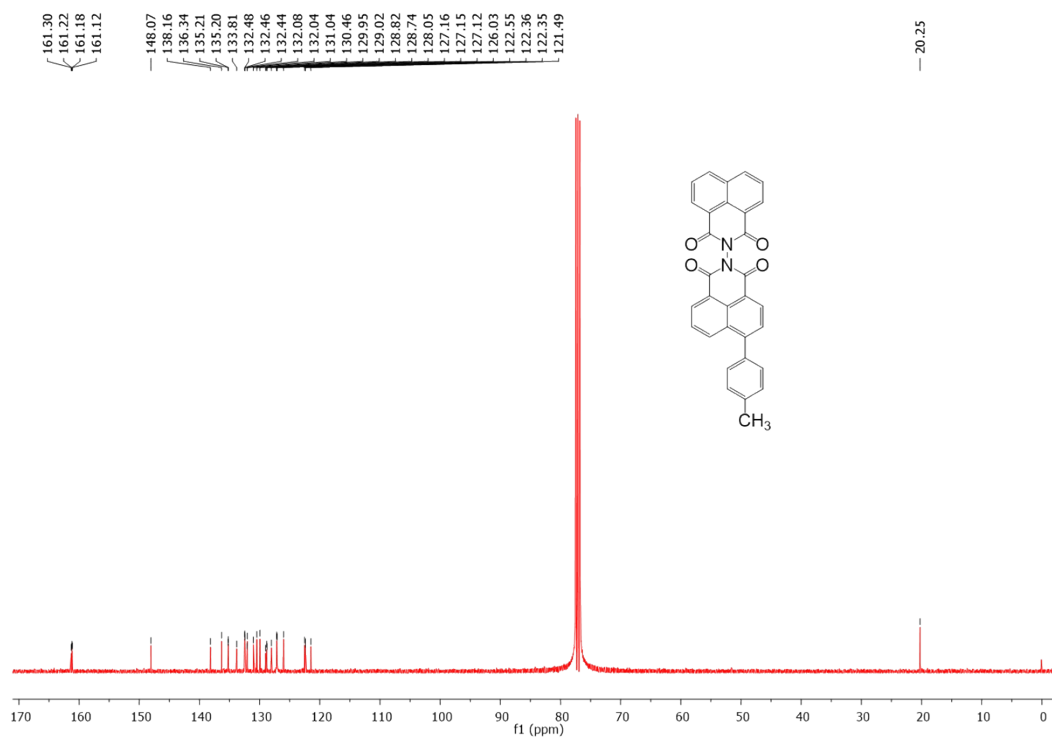


Figure S24. ¹³C NMR spectrum of 6-(*p*-tolyl)-1*H*,1'*H*,3*H*,3'*H*-[2,2'-bibenzo[*de*]isoquinoline]-1,1',3,3'-tetraone (**5k**)

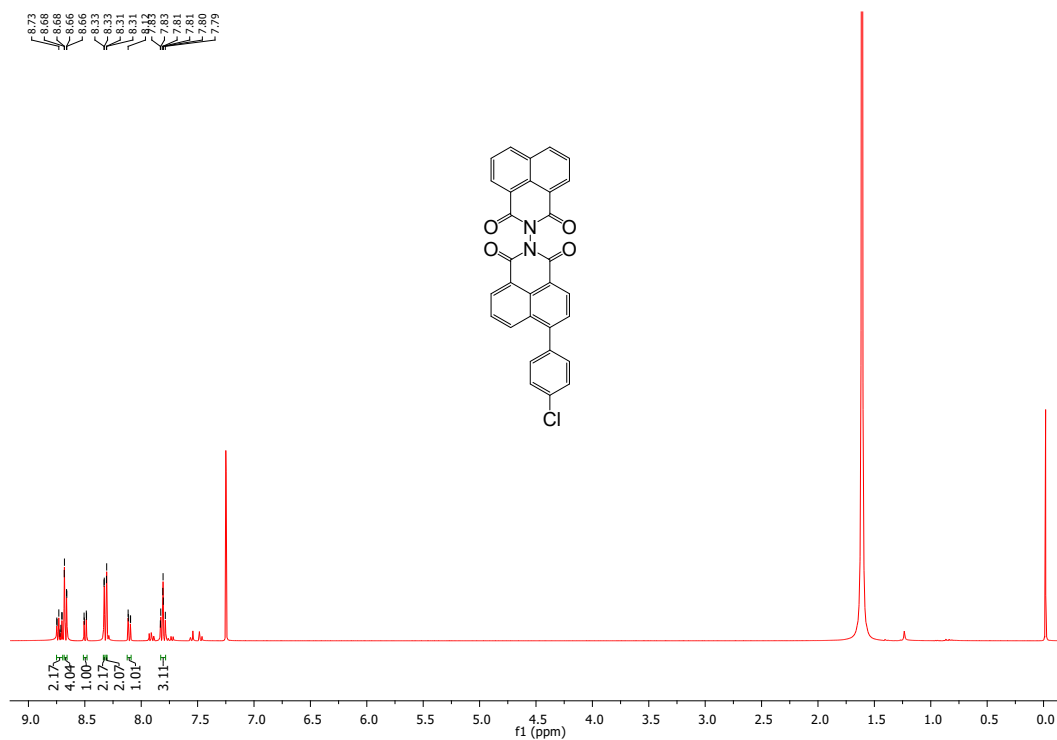


Figure S25. ^1H NMR spectrum of 6-6-(4-chlorophenyl)-1*H*,1'*H*,3*H*,3'*H*-[2,2'-bibenzo[*de*]isoquinoline]-1,1',3,3'-tetraone (**51**)

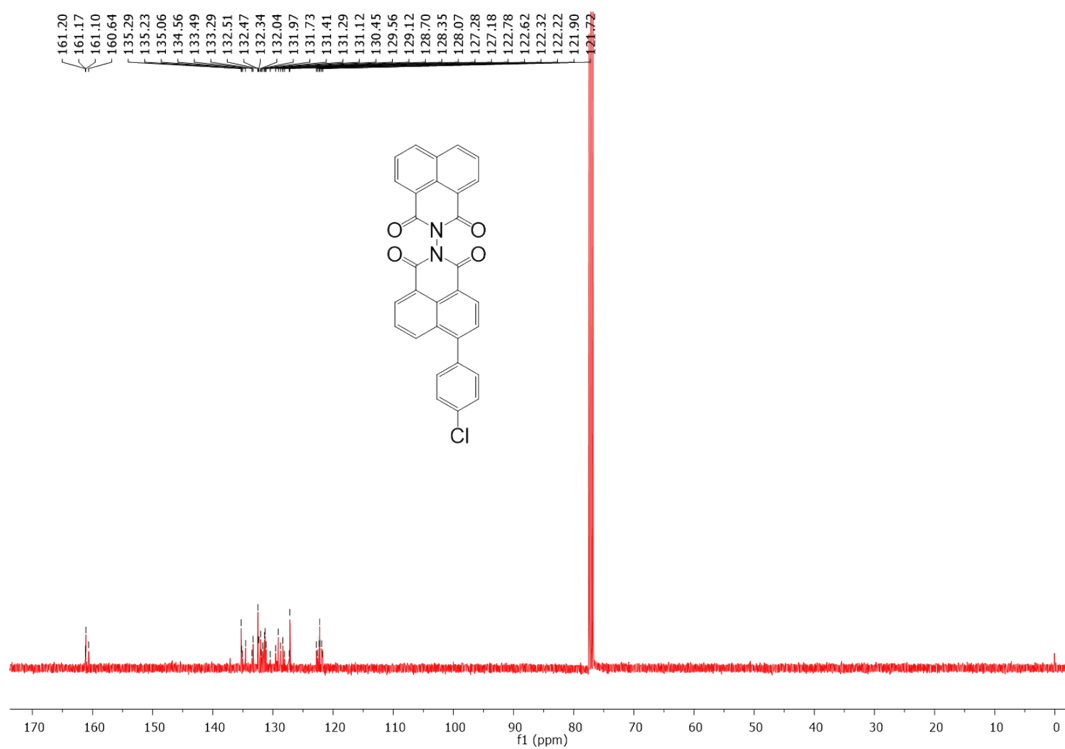


Figure S26. ^{13}C NMR spectrum of 6-6-(4-chlorophenyl)-1*H*,1'*H*,3*H*,3'*H*-[2,2'-bibenzo[*de*]isoquinoline]-1,1',3,3'-tetraone (**51**)

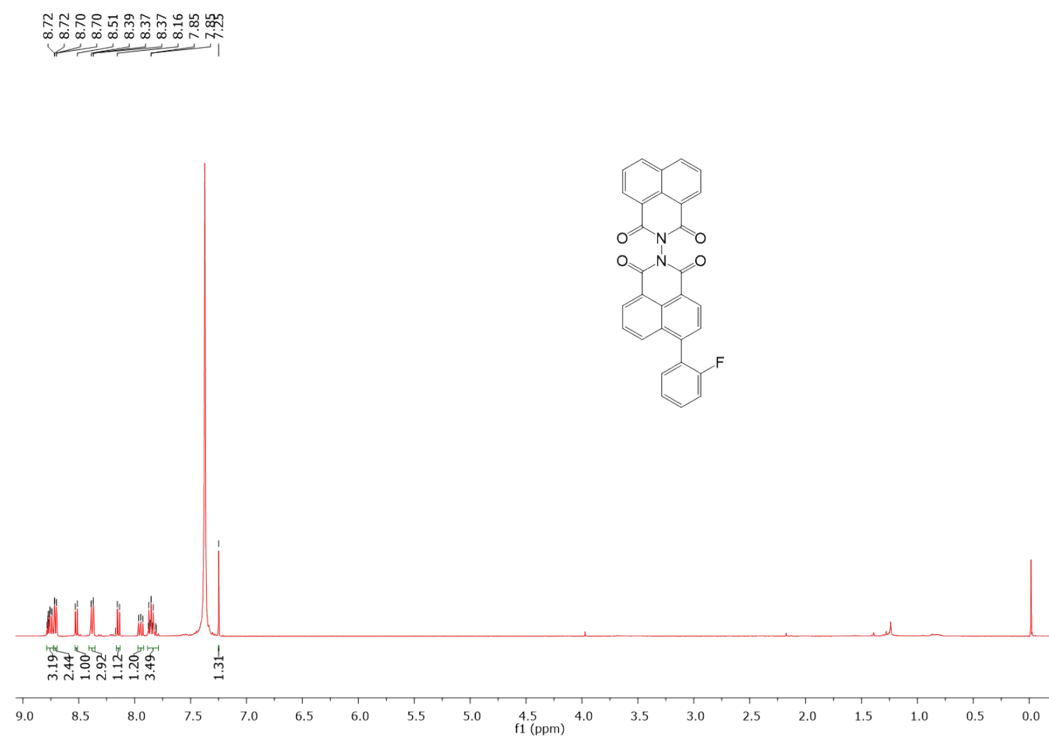


Figure S27. ^1H NMR spectrum of 6-(2-fluorophenyl)-1*H*,1'*H*,3*H*,3'*H*-[2,2'-bibenzo[*de*]isoquinoline]-1,1',3,3'-tetraone (**5m**)

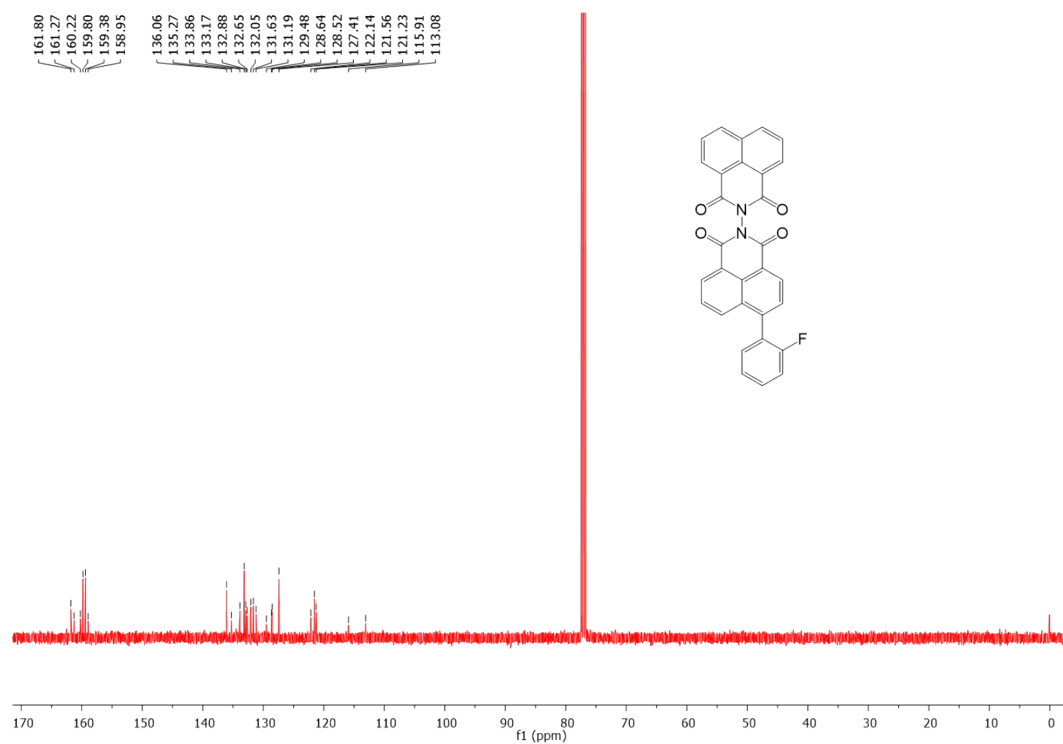


Figure S28. ^{13}C NMR spectrum of 6-(2-fluorophenyl)-1*H*,1'*H*,3*H*,3'*H*-[2,2'-bibenzo[*de*]isoquinoline]-1,1',3,3'-tetraone (**5m**)

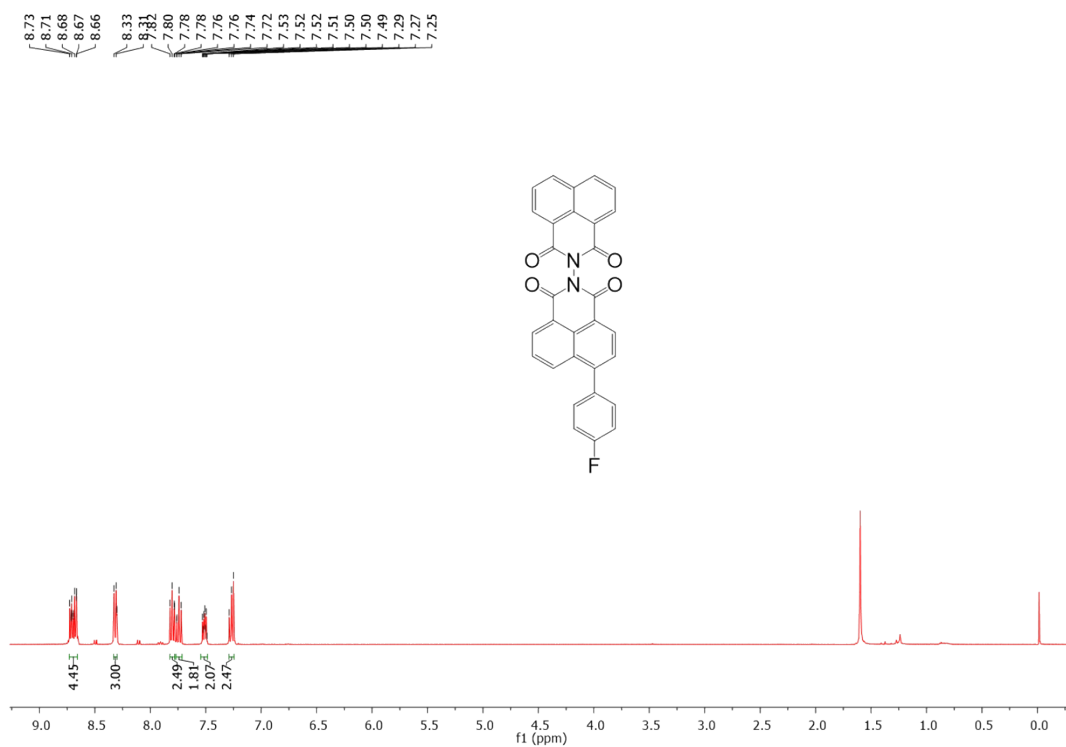


Figure S29. ^1H NMR spectrum of 6-(4-fluorophenyl)-1*H*,1'*H*,3*H*,3'*H*-[2,2'-bibenzo[*de*]isoquinoline]-1,1',3,3'-tetraone (**5n**)

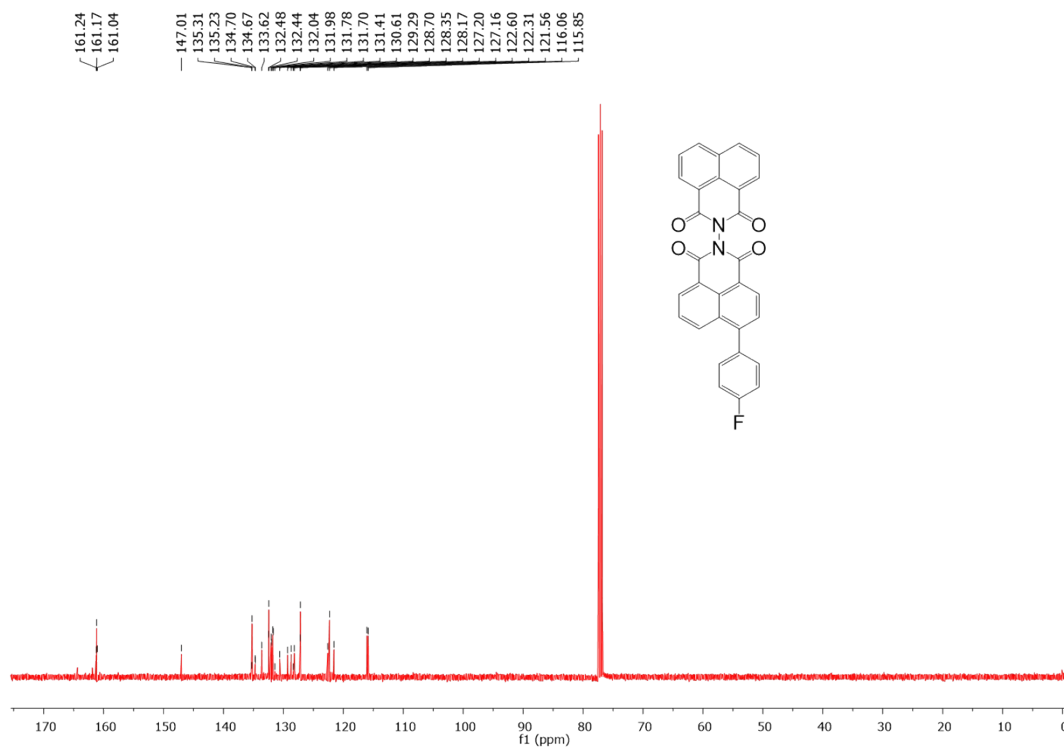


Figure S30. ^{13}C NMR spectrum of 6-(4-fluorophenyl)-1*H*,1'*H*,3*H*,3'*H*-[2,2'-bibenzo[*de*]isoquinoline]-1,1',3,3'-tetraone (**5n**)

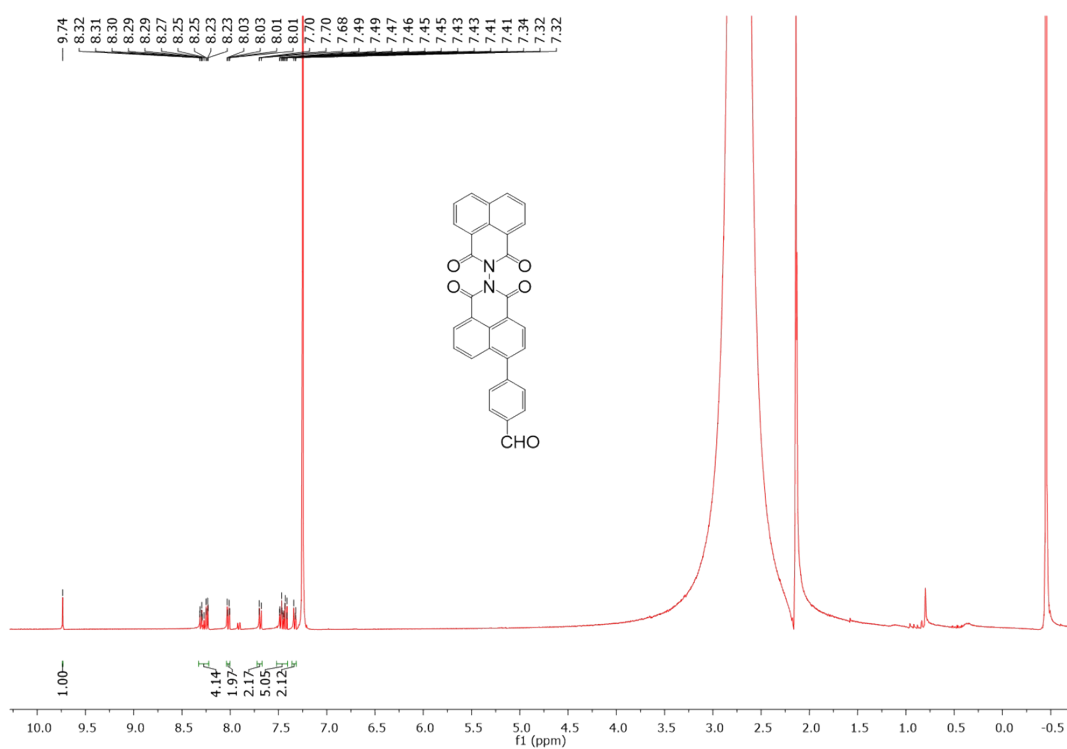


Figure S31. ^1H NMR spectrum of 4-(1,1',3,3'-tetraoxo-1*H*,1'*H*,3*H*,3'*H*-[2,2'-bibenzo[*de*]isoquinolin]-6-yl)benzaldehyde (**5o**)

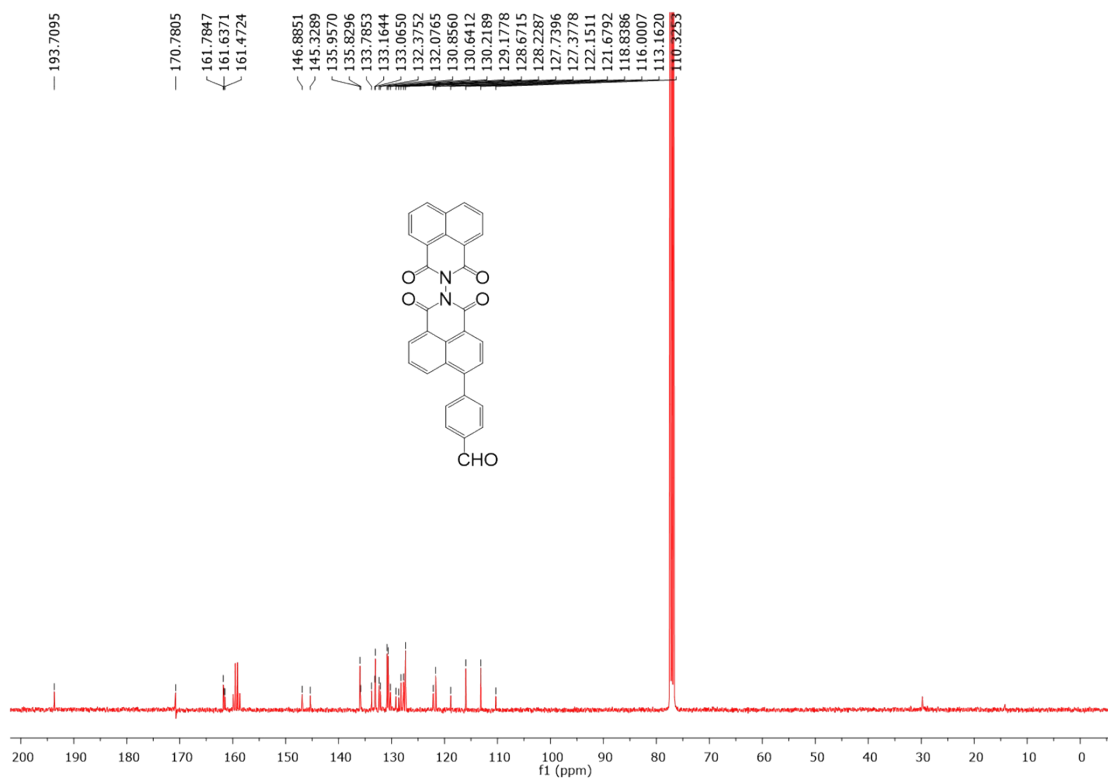


Figure S32: ^1H NMR spectrum of 4-(1,1',3,3'-tetraoxo-1*H*,1'*H*,3*H*,3'*H*-[2,2'-bibenzo[*de*]isoquinolin]-6-yl)benzaldehyde (**5o**)

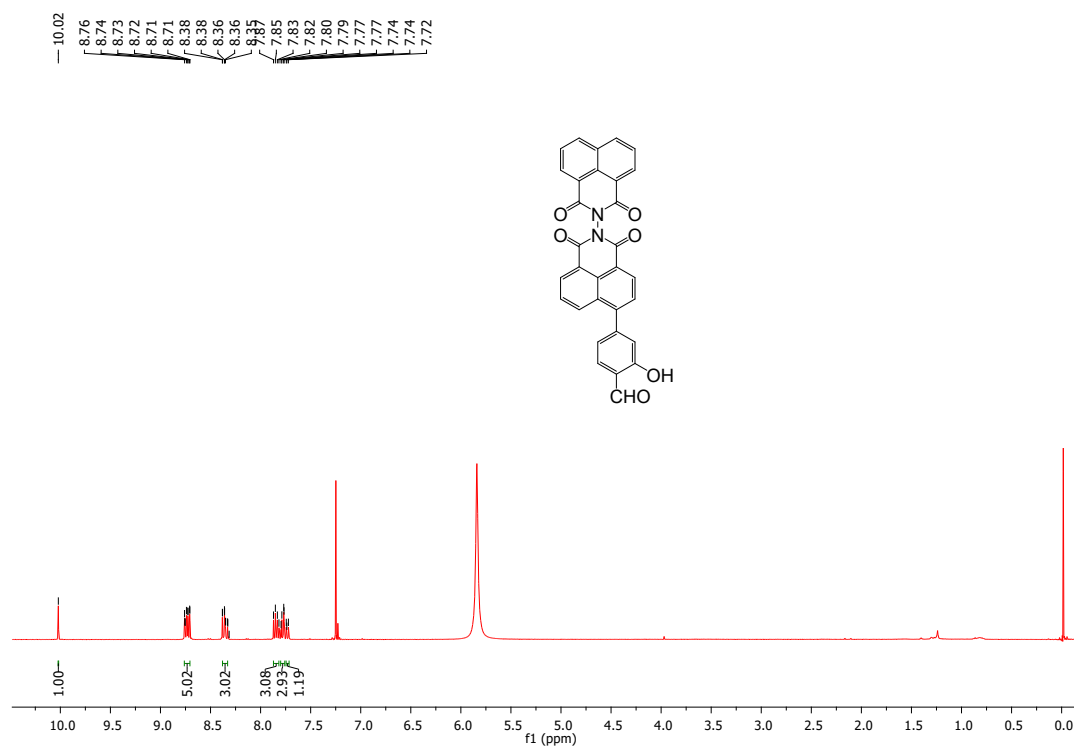


Figure S33. ^1H NMR spectrum of 2-hydroxy-5-(1,1',3,3'-tetraoxo-1*H*,1'*H*,3*H*,3'*H*-[2,2'-bibenzo[*de*]isoquinolin]-6-yl)benzaldehyde (**5p**)

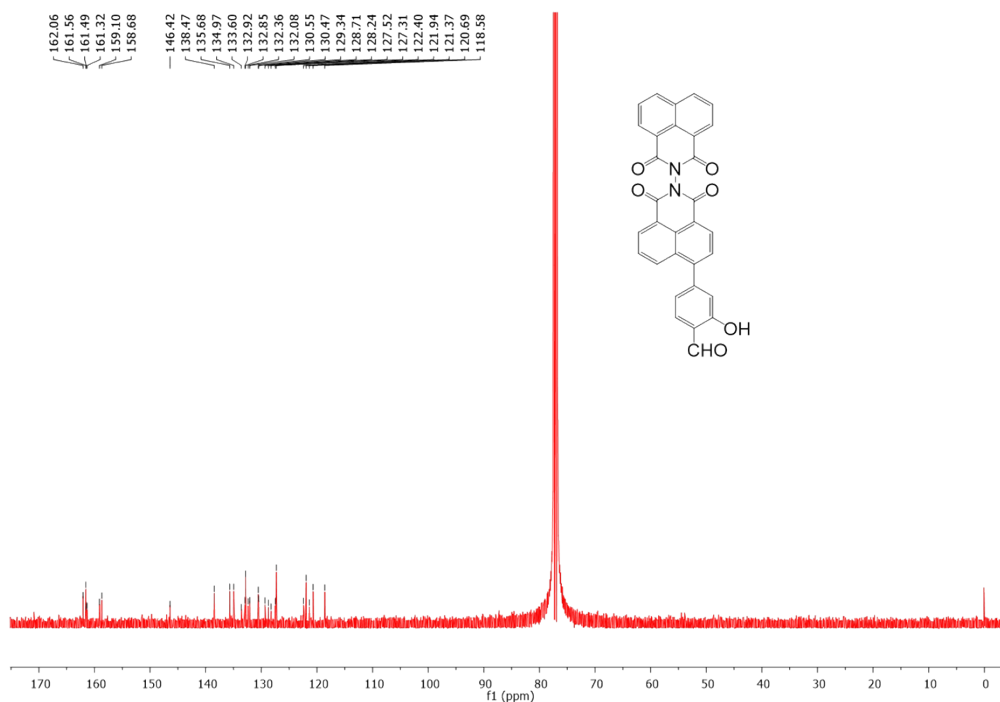


Figure S34. ^{13}C NMR spectrum of 2-hydroxy-5-(1,1',3,3'-tetraoxo-1*H*,1'*H*,3*H*,3'*H*-[2,2'-bibenzo[*de*]isoquinolin]-6-yl)benzaldehyde (**5p**)

Biological assays

Minimal inhibitory concentration (MIC, $\mu\text{g}/\text{mL}$) is defined as the lowest concentration of target compounds that ultimately inhibit the growth of bacteria, using a standard two-fold serial dilution method in 96-well micro test plates according to the National Committee for Clinical Laboratory Standards (NCCLS). The tested bacterial strains were purchased from the Institute of Microbial Technology (IMTech), Chandigarh. Chloromycin, tetracycline, and amoxicillin were used as control drugs. DMSO was inoculated with bacteria having no medicine as a positive control to check the effect of solvent bacterial growth. All the bacteria growth was monitored visually and spectrophotometrically, and the experiments were performed in triplicate.

Antibacterial assays

The synthesized compounds **5a-5p** were examined for their antibacterial activities against four Gram-positive bacteria viz (*Staphylococcus aureus* (MTCC No-902), *Enterococcus faecalis* (MTCC No-6845), *Bacillus subtilis* (MTCC No- 441), *Listeria* (MTCC No- 4214) and four Gram-negative bacteria such as *Escherichia coli* (MTCC No-448), *Salmonella enterica* (MTCC No-1165), *Acinetobacter calcoaceticus* (MTCC No-1948), *Serratia marcescens*

(MTCC No-2645). The bacterial suspension was adjusted with sterile saline to a concentration of 1×10^5 CFU/mL. The stock solutions were prepared by dissolving compounds in DMSO. The compounds and reference drugs were prepared in Nutrient broth by two-fold serial dilution to obtain the required concentrations of 800, 400, 200, 100, 50, 25, 12.5, 6.25, 3.125, 1.56 $\mu\text{g/mL}$. These dilutions were inoculated and incubated at 37 °C for 24 h.

Minimal bactericidal concentrations (MBC) assays

The broth microdilution assay determined minimal bactericidal concentrations (MBC) for **5d** and **5o** against *E. faecalis*. These compounds were 2-fold serially diluted and incubated with *E. faecalis* in a 96-well plate according to the procedure outlined for MIC determination. After 24 h incubation period, 50 μl of the suspension from the microwell plate was plated onto tryptic soy agar (TSA). The lowest concentration showing no visible growth on the scale was considered the MBC value.

Bacterial Susceptibility Evaluation

After determining the MIC values, multiple passaging was performed by transferring bacterial suspension grown at sub-MIC. After the growth of *E. faecalis*, new MIC value was calculated towards each passage of the strain; tetracycline and amoxicillin were taken as controls. The experiment was continued for 20 days.

Drug combination Assay

The drug combination effects of **5d** and **5o** with standard drugs tetracycline and amoxicillin towards various bacterial strains were performed using standard checkboard assay.¹

Table S1. Combination effect of **5d** and **5o** with tetracycline and amoxicillin against *B. subtilis*

	5d	Tetra	Amox	5o	Terta	Amox
MIC	400	1.56	50	1.56	1.56	50
MIC comb.	200	0.78	50	0.39	0.19	25
FIC	0.5	0.5	1	0.25	0.12	0.5
FIC Index	1.0		1.5	0.37		0.75
Effect	additivism	additivism		Synergistic		Additivism

Table S2. Combination effect of **5d** and **5o** with tetracycline and amoxicillin against *L. species*

	5d	Tetra	Amox	5o	Terta	Amox
MIC	25	6.25	50	1.56	6.25	50
MIC comb.	3.12	0.78	50	0.19	1.56	18.5
FIC	0.12	0.12	1	0.12	0.24	0.37
FIC Index	0.24		1.12	0.36		0.49
Effect	Synergistic		Additivism	Synergistic		Additivism

Table S3. Combination effect of **5d** and **5o** with tetracycline and amoxicillin against *S. aureus*

	5d	Tetra	Amox	5o	Terta	Amox
MIC	1.56	1.56	25	3.12	1.56	25
MIC comb.	0.23	0.14	12.6	0.75	0.13	14.5
FIC	0.14	0.08	0.50	0.24	0.08	0.58
FIC Index	0.22		0.64	0.32		0.82
Effect	Synergistic		Additivism	Synergistic		Additivism

Table S4. Combination effect of **5d** and **5o** with tetracycline and amoxicillin against *E. coli*

	5d	Tetra	Amox	5o	Terta	Amox
MIC	1.56	1.56	100	200	1.56	100
MIC comb.	0.13	0.39	50	50	0.39	50
FIC	0.08	0.25	0.50	0.25	0.25	0.5
FIC Index	0.33		0.58	0.5		0.75
Effect	Synergistic		Additivism	Additivism		Additivism

Table S5. Combination effect of **5d** and **5o** with tetracycline and amoxicillin against *S. enterica*

	5d	Tetra	Amox	5o	Terta	Amox
MIC	3.12	100	200	6.25	100	200
MIC comb.	0.39	25	100	0.78	12.5	100
FIC	0.12	0.25	0.50	0.12	0.12	0.50
FIC Index	0.37		0.75	0.24		0.62
Effect	Synergistic		Additivism	Synergistic		Additivism

Table S6. Combination effect of **5d** and **5o** with tetracycline and amoxicillin against *A. calcoaceticus*

	5d	Tetra	Amox	5o	Terta	Amox
MIC	200	1.56	50	3.12	1.56	50
MIC comb.	100	0.52	25	0.55	0.24	14.5
FIC	0.5	0.33	0.50	0.17	0.15	0.58
FIC Index	0.83		1.0	0.32		0.75
Effect	Additivism	Additivism	Additivism	Synergistic	Additivism	Additivism

Table S7. Combination effect of **5d** and **5o** with tetracycline and amoxicillin against *S. marcescens*

	5d	Tetra	Amox	5o	Terta	Amox
MIC	3.12	1.56	1.56	1.56	1.56	1.56
MIC comb.	0.78	0.19	0.78	0.19	0.39	1.56
FIC	0.25	0.12	0.50	0.12	0.25	1
FIC Index	0.37		0.62	0.37		1.12
Effect	Synergistic	Additivism	Additivism	Synergistic	Additivism	Additivism

Time-killing kinetics of *Enterococcus faecalis*

E. faecalis cells were incubated with compounds **5d** and **5o** at different concentrations (MIC, 2 MIC, 4 MIC, 8 MIC) in a 96-well plate at 37 °C. The absorbance values of untreated and treated cells were recorded for 6 h at an interval of 30 min, using an Elisa plate reader (Biotek, Power-Wave XS2). The decrease in value of absorbance was noted.

Cytotoxicity towards cancer cell lines

Cytotoxicity of derivatives was examined at the National Cancer Institute (NCI), USA, following their standard procedure.²

Cytotoxicity toward a normal cell line

Human embryonic kidney (Hek293) cells were cultured in DMEM with 10% FBS, 50 mM glutamine, 100 mg/ml streptomycin, and 100 U/ml penicillin. Cells were seeded in

two 96 well plates at the density of 1×10^{-5} cells/well in DMEM media supplemented with 10% FBS cells. Cells were incubated at 37 °C in a 5% CO₂ incubator. Cells were treated with compounds **5d** and **5o** at five concentrations (0.78, 1.56, 3.125, 6.25, 12.5 µg/ml) at 37 °C for 48 h. 10 µl of MTT (prepared in 1* PBS buffer) from 5 mg/ml stock was added in each well and incubated at 37 °C for 4 h in the dark. The formazan crystals were dissolved using 100 µl of DMSO. Further, the amount of formazan crystal formation was measured as the difference in absorbance by Bio-Tek ELISA plate reader at 570 nm reference wavelength. All experiments were independently performed at least three times. The relative cell toxicity (%) related to control wells containing culture medium without test material was calculated using the following formula (Eq. (1))

$$\% \text{ Cell Toxicity} = 100 - \frac{OD (\text{compound treated wells})}{OD (\text{untreated wells})} \times 100 \quad (1)$$

Table S8: Cytotoxicity of derivatives **5a-5h** at 20 µg/ml concentration

	5a	5b	5c	5d	5e	5f	5g	5h
Leukaemia								
CCRF-CEM	-	-	32.36	50.47	-	-	-	10.91
HL-60(TB)	-	-	-	-	-	-	35.25	-
K-562	-	-	42.89	61.11	11.6	14.53	-59.25	12.8
MOLT-4	-	-	7.12	11.04	0.75	-	38.5	10.44
SR	-	-	55.85	50.39	10.63	9.26	-6.4	9.76
RPMI-8226	-	-	-	-	-	-	-	-
Lung Cancer								
A549	-	1.83	-	-	-	0.76	10.12	5.59
EKVX	6.99	7.15	5.98	6.88	7.71	18.84	2.09	10.68
HOP-62	6.34	3.68	-	1.99	0.04	10.83	11.07	7.45
HOP-92	19.62	1.34	6.13	13.27	12.35	15.2	21.85	20.13
NCI-H226	6.43	6.11	-	-	6.04	13.16	1.43	6
NCI-H23	3.85	8.12	1.82	2.3	2.16	11.57	7.76	9.59
NCI-H322M	7.74	-	1.84	4.49	7.85	12.93	11.81	3.62
NCI-H460	-	-	1.67	-	-	0.98	27.65	1.9
NCI-H522	4.51	6.06	-	0.1	2.46	6.26	6.18	11.91
Colon Cancer								
COLO 205	-	-	-	-	-	-	4.81	-
HCC-2998	-	-	-	-	-	-	2.57	-
HCT-116	-	0.35	-	-	2.09	2.26	41.89	1.1
HCT-15	-	-	-	2.75	2.14	2.62	49.4	3.41
HT29	0.35	-	-	0.73	-	-	12.72	4.08
KM12	1.1	-	1.18	2.89	0.44	1.46	17.82	0.55
SW-620	2.85	-	2.71	0.29	5.02	5.25	21.34	1.3
CNS Cancer								
SF-268	1.96	1.88	3.71	6.19	1.27	2.78	11.28	6.37
SF-295	-	-	-	-	-	0.56	-	4.75
SF-539	3.77	0.24	10.75	-	1.58	-	-	5.81
SNB-19	0.81	0.68	0.83	0.53	4.21	2.51	11.47	10.93
SNB-75	1.12	9.58	7.57	15.69	7.97	13.82	7.76	12.49

U251	1.39	4.56	-	-	-	1.15	13.73	0.3
Melanoma								
LOX IMVI	4.13	9.19	5.25	5.7	4.7	8.34	13.52	7.87
MALME-3M	4.67	-	3.25	3.15	10.5	13.78	11.07	9.17
M14	5.71	-	-	-	4.64	7.19	3.37	3.81
MDA-MB-435	-	-	-	-	-	-	0.12	-
SK-MEL-2	-	-	-	-	-	-	-	-
SK-MEL-28	-	-	-	-	-	-	-	-
SK-MEL-5	1.3	-	-	-	1.31	3.97	7.18	3.29
UAAC-257	-	1.54	-	-	-	2.8	4.78	-
UAAC-62	6.61	4.34	-	0.63	8.1	9.71	4.29	16.47
Ovarian Cancer								
IGROV1	-	-	0.68	5.16	2.94	23.95	8.78	-
OVCAR-3	-	-	-	-	-	-	-	-
OVCAR-4	-	-	-	-	0.74	2.92	-	3.17
OVCAR-5	-	-	-	-	-	-	-	9.43
OVCAR-8	1.72	-	-	5.55	1.77	3.23	17.4	3.77
NCI-RES	2.75	-	-	0.74	0.26	7.83	17.39	4.59
SK-OV-3	1.28	-	0.27	5.09	0.96	10.36	-	7.94
Renal Cancer								
786-0	-	-	0.75	2.88	-	-	26.29	-
A498	-	-	8.75	3.19	-	-	24.91	4.52
ACHN	-	-	3.51	1.5	10.04	7.14	12.2	7.82
CAKI-1	15.57	5.88	13.09	14.1	19.09	19.21	7.64	20.11
RXF 393	-	-	-	-	-	-	-	7.1
SN12C	5.86	-	0.85	3.43	5.45	3.95	10.17	8.26
TK-10	-	-	-	-	-	-	-	-
UO-31	17.92	18.92	20.04	19.08	22.78	31.44	28.44	33.74
Prostate cancer								
PC-3	8.22	-	8.85	7.17	9.59	12.31	14.93	16.38
DU-145	-	-	-	-	-	-	-	-
Breast Cancer								
MCF7	5.17	12.63	1.97	1	2.28	8.31	70.98	11.18
MDA-MB-231	6.16	-	-	5.66	14.65	20.27	14.22	24.36
HS 578T	-	2.78	7.37	9.17	3.87	-	14.12	-
BT-549	-	-	-	-	-	-	10.18	2.23
T-47D	5.96	3.5	2.26	1.44	1.64	13.76	6.39	11.56
MDA-MB-468	-	-	-	-	0.69	-	9.03	-

Table S9: Cytotoxicity of derivatives **5i-5p** at 20 $\mu\text{g/ml}$ concentration

	5i	5j	5k	5l	5m	5n	5o	5p
Leukaemia								
CCRF-CEM	3.18	-	-	-	-	-	-	18.54
HL-60(TB)	-	-	-	-	-	-	-	5.78
K-562	13.59	-	-	1.39	10.16	-	3.72	31.05
MOLT-4	-	-	-	-	-	-	-	-
SR	-	2.17	-	39.57	68.17	-	-	5.36
RPMI-8226	70.59	-	3.69	-	12.18	-	5.62	7.58
Lung Cancer								
A549	-	-	-	-	-	-	-	-
EKVX	10.58	13.63	5.71	-	-	1.98	10.91	1.69
HOP-62	7.28	8.96	-	-	-	-	3.83	4.79
HOP-92	24.36	11.24	6.43	-	-	7.36	13.71	18.3
NCI-H226	-	-	-	-	-	-	-	-
NCI-H23	3.89	-	-	-	-	-	-	-
NCI-H322M	-	-	-	-	-	3.21	-	-
NCI-H460	-	-	-	-	-	-	-	-

NCI-H522	2.94	-	-	-	-	-	-	-
Colon Cancer								
COLO 205	-	-	-	-	-	-	-	-
HCC-2998	-	-	-	-	-	-	-	-
HCT-116	3.16	1.42	-	-	7.22	-	1.33	6.92
HCT-15	-	3.4	-	-	-	1.82	-	10.6
HT29	-	-	-	-	-	-	-	-
KM12	3.78	-	-	2.62	-	30.73	-	-
SW-620	-	-	-	-	-	-	-	-
CNS Cancer								
SF-268	2.29	-	-	-	-	-	-	3.57
SF-295	-	-	-	-	-	-	-	-
SF-539	4.3	4	-	-	2.28	3.97	-	10.9
SNB-19	-	-	5.1	-	-	-	1.51	-
SNB-75	3.67	24.28	-	16.33	13.08	8.26	18.94	21.95
U251	26.89	-	13.87	-	-	-	-	8.64
Melanoma								
LOX IMVI	-	-	-	-	-	-	-	-
MALME-3M	6.93	-	-	-	3.46	-	7.23	3.43
M14	5.81	2.29	-	3.05	-	-	7.33	-
MDA-MB-435	1.18	-	-	-	-	-	-	-
SK-MEL-2	-	-	-	-	-	-	-	-
SK-MEL-28	-	-	-	-	-	-	-	-
SK-MEL-5	-	-	-	-	-	-	1.51	-
UAAC-257	-	-	-	-	-	-	-	-
UAAC-62	3.16	-	-	-	-	-	-	-
Ovarian Cancer								
IGROV1	7.55	1.06	-	-	-	-	6.21	5.68
OVCAR-3	-	-	-	-	-	-	-	-
OVCAR-4	2.51	-	-	-	-	-	2.98	-
OVCAR-5	-	-	-	-	-	-	-	-
OVCAR-8	-	-	-	-	-	-	-	1.18
NCI-RES	1.76	-	-	-	-	-	-	-
SK-OV-3	-	-	-	-	-	-	-	-
Renal Cancer								
786-0	-	-	-	-	3.62	-	-	-
A498	-	-	-	-	-	-	3.19	-
ACHN	3.69	-	-	-	-	-	-	3.41
CAKI-1	24.82	20.8	12.89	9.01	10.83	16.65	14.23	23.18
RXF 393	-	-	-	-	-	-	-	-
SN12C	-	4.03	-	-	-	-	-	7.04
TK-10	-	-	-	-	-	-	-	-
UO-31	31.41	28.25	16.04	-	19.07	22.88	20.31	29.02
Prostate cancer								
PC-3	12.34	11.68	-	-	-	-	2.02	10.81
DU-145	-	-	-	-	-	-	-	-
Breast Cancer								
MCF7	84.3	8.55	-	58.04	89.48	12.02	1.48	6.97
MDA-MB-231	16.34	2.62	-	-	-	-	7.92	5.45
HS 578T	-	3.65	-	73.82	-	-	-	3.2
BT-549	-	-	-	-	-	-	-	-
T-47D	2.02	-	-	-	8.56	-	-	6.18
MDA-MB-468	3.54	-	-	-	-	-	2.58	-

-- indicates the percentage of growth > 100

Anti-biofilm Assay

The bacterial suspension of *E. faecalis* was incubated with compounds **5d** and **5o** at different concentrations in a 96-well plate for 72 h at 37 °C. The culture supernatant was discarded, and the sediment was washed with phosphate buffer. Then the plate was incubated for 1 h at 60 °C to fix the biofilm. After incubating for 1 h, crystal violet dye (0.1%) was added to the stain for 1 h at room temperature. The excess dye was discarded and then rinsed with distilled water. Finally, 33% acetic acid was used to elute the stained biofilm. The absorbance was noted at 600 nm in a microplate reader.

Outer membrane disruption

The grown culture of *E. faecalis* was harvested at 3500 rpm for 5 – 10 min, washed, and suspended in a mixture of 5 mM glucose and 5mM Hepes buffer (1:1) at pH 7.2 to give a value of 10⁸ CFU/ml. 150 µL of this bacterial suspension was transferred to 96 well plates and 50 µL NPN dye (10 µM) was added to the well, and the plate was incubated for 1 h. Fluorescence intensity was measured using a fluorescence spectrophotometer at an excitation wavelength of 350 nm and emission wavelength of 420 nm for 30 min (control group). Further compounds **5d** and **5o** were added, and the intensity of fluorescence was noted at various concentrations (1,2,4,8 × MIC) under same conditions. Dimethyl sulfoxide was used as a negative control, and experiments were repeated in triplicates.

Inner membrane disruption

The grown culture of *E. faecalis* was harvested at 3500 rpm for 5 – 10 min, washed, and suspended in a mixture of 5 mM glucose and 5 mM Hepes buffer (1:1) at pH 7.2 to give a value of 10⁸ CFU/ml. 150 µL of this bacterial suspension was transferred to 96 well plates, and 50 µL EtBr dye (10µM) was added to the well, and the plate was incubated for 30 min. Fluorescence intensity was measured using a fluorescence spectrophotometer at an excitation wavelength of 520 nm and emission wavelength of 610 nm for 30 min (control group). Further compounds **5d** and **5o** were added, and the fluorescence intensity was noted at various concentrations (1,2,4,8 × MIC) under the same conditions. Dimethyl sulfoxide was used as a negative control, and the experiment was repeated in triplicates.

Leakage of intercellular protein

The grown culture of bacteria *E. faecalis* was incubated with increasing concentrations of compounds **5d** and **5o** (1, 2, 4,8 ×MIC) for 24 h. Then, the mixture was centrifuged at 3500

rpm for 10 min, and the supernatant was collected. The concentration of the leaked protein in the supernatant was determined by standard follin assay.

Metabolic activity

The bacterial culture of *E. faecalis* was treated with increasing concentrations of compounds **5d** and **5o** for 6h at 37 °C. The untreated and treated cells were incubated with resazurin dye (50 µg/ml, 25 µl) for 1 h at 37 °C, and then the absorbance was measured at 570 nm on an Elisa plate reader. The average % reduction was used to determine the metabolic activity.

Scanning electron microscopy

The bacteria *E. faecalis* was centrifuged at 3500 rpm for 5 min, and the supernatant was discarded. The bacteria cell was washed with PBS and suspended with PBS. The bacterial suspension was incubated with compounds **5d** and **5o** (2 × MIC) for 6h at 37 °C and centrifuged at 3500 rpm for 5 min and then washed thrice with PBS. The cells were fixed with 2.5 % glutaraldehyde overnight at 4 °C and washed with PBS buffer and dehydrated with different concentrations of ethanol (45, 55, 65, 75, 95 and 100%). Then, the pellet was transferred to silicon chip and dried. The samples were coated with gold and visualized under a scanning electron microscope.

Reactive Oxygen Species (ROS) production

Intracellular ROS was measured using a standard 2,7-dichlorofluorescein diacetate (DCFH-DA) assay. Then, 10⁶ CFU/mL of *E. faecalis* cells were treated with increasing concentrations of compounds **5d** and **5o** for 6 h at 37 °C. Following treatment, both control and treated cells were harvested and washed with PBS, followed by incubation with 100 µM DCFH-DA probe for 30 min in dark at 37 °C. The fluorescence originating from the oxidative cleavage of DCFH-DA to DCF was measured with a fluorescence spectrophotometer with an excitation wavelength of 485 nm and an emission wavelength of 528 nm. The increase in intracellular ROS production in cells treated with compounds **5d** and **5o** compared to control cells was plotted.

Intracellular Glutathione (GSH) activity

The activity of intracellular GSH was determined using a standard Ellman's assay. The *E. faecalis* suspensions (~10⁵ CFU/mL) were treated with increasing concentrations of compounds for 6 h at 37 °C. Both control and treated cells were centrifuged at 5000 rpm for 5 min, washed with PBS, and lysed. The clear supernatant was collected. Then, the Tris-HCl (50 mM) and 5,5-dithiobis (2-nitrobenzoic acid) (DTNB) (100 mM) were added and incubated for

30 min in dark at 37 °C. The resulting solution was measured at 412 nm by spectrophotometry (eq 2).

$$\left(1 - \frac{\text{OD@412 nm of treated}}{\text{OD@412 nm of control}}\right) \times 100 \quad (2)$$

Lipid peroxidation

Malondialdehyde (MDA) is a natural product of lipid oxidation in organisms. Some aliphatic acids are gradually decomposed into complex compounds after oxidation, including MDA. Therefore, the level of lipid oxidation can be detected by detecting the level of MDA. The *E. faecalis* suspensions ($\sim 10^5$ CFU/mL) were treated with increasing concentrations of compounds for 4 h at 37 °C. Under the dark condition, trichloroacetic acid (TCA) was added to stop the reaction and then 0.5% thiobarbituric acid was added. The mixture was heated at 80 °C for 0.5 h. After using an ice bath to cool the mixture, both control and treated cells were centrifuged at 5000 rpm for 5 min, and then collected the supernatant and tested by a microplate reader at 535 nm.

Hemolysis Assay

The goat red blood cells (RBCs) were collected and washed three times with saline. Subsequently, the cells were reallocated in saline to provide 5% V/V red blood cell suspension. The RBCs suspension (400 μ L) was added to a 1.5 ml centrifuge tube containing 400 μ L of 2-fold serially diluted compound **5d** and **5o** solution and incubated for 3h at 37 °C. The mixture was centrifuged at 2000 rpm for 5 min, and the supernatant (100 μ L) was removed to a new 96-well plate. The absorbance of the supernatant was measured at 540 nm using a microplate reader. 1% Triton X-100 and saline were used as positive and negative controls, respectively. The hemolytic activity was calculated by the following equation: hemolysis (%) = $[(\text{OD}_{\text{sample}} - \text{OD}_{\text{saline}}) / (\text{OD}_{\text{Triton X-100}} - \text{OD}_{\text{saline}})] \times 100\%$. The experiment was performed in triplicate.

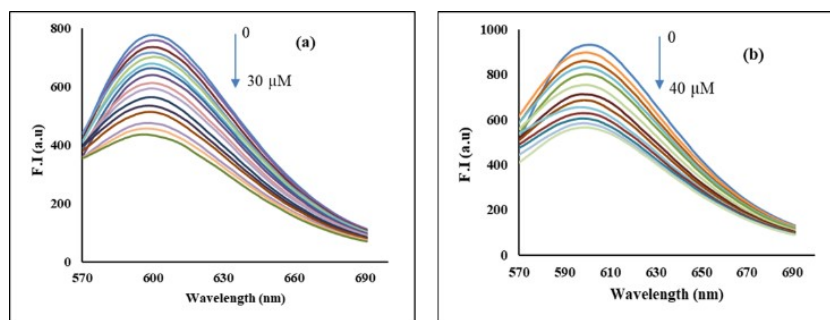
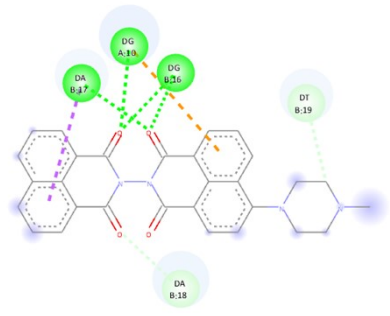
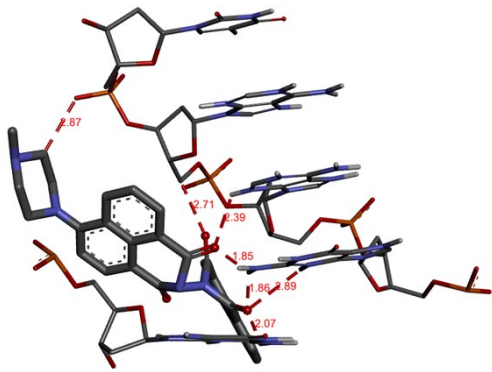


Figure S35: Fluorescence spectra of ethidium bromide and ct-DNA complexes upon gradual addition of compounds (a) **5d** (0–30 μM) and (b) **5o** (0–40 μM)

Table S10: Docked pose of compounds into 3D crystal structure of DNA and 2D representations

Compound	Docked pose of compounds into 3D crystal structure of DNA	2D-representation
5a		<p>Interactions</p> <ul style="list-style-type: none"> Conventional Hydrogen Bond (Green circle) Carbon Hydrogen Bond (Light Green circle) Pi-Anion (Orange circle) Pi-Sigma (Purple circle)
5b		<p>Interactions</p> <ul style="list-style-type: none"> Conventional Hydrogen Bond (Green circle) Carbon Hydrogen Bond (Light Green circle) Pi-Anion (Orange circle) Pi-Sigma (Purple circle)

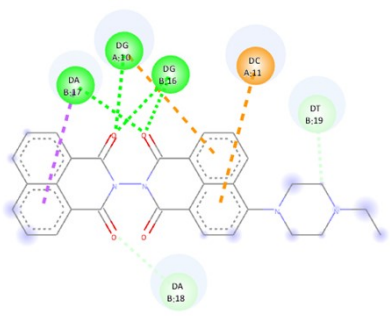
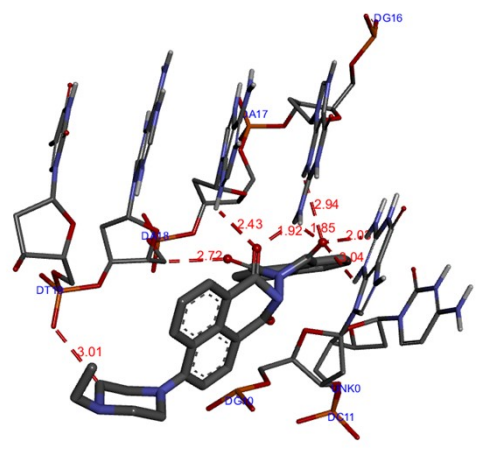
5c



Interactions

	Conventional Hydrogen Bond		Pi-Anion
	Carbon Hydrogen Bond		Pi-Sigma

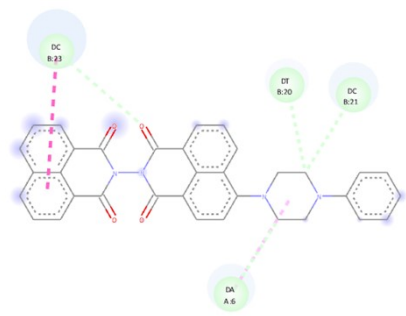
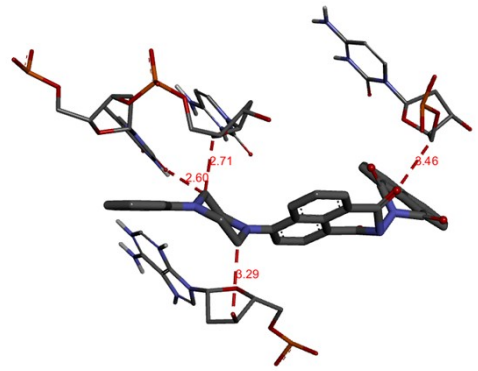
5d



Interactions

	Conventional Hydrogen Bond		Pi-Anion
	Carbon Hydrogen Bond		Pi-Sigma

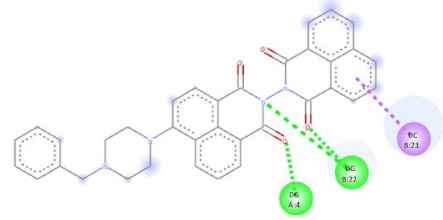
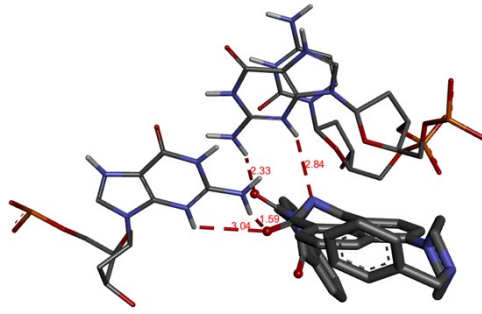
5e



Interactions

	Carbon Hydrogen Bond		Pi-Alkyl
	Pi-Pi Stacked		

5f



Interactions

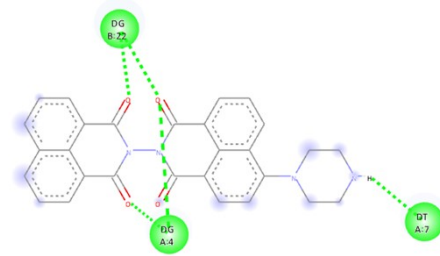
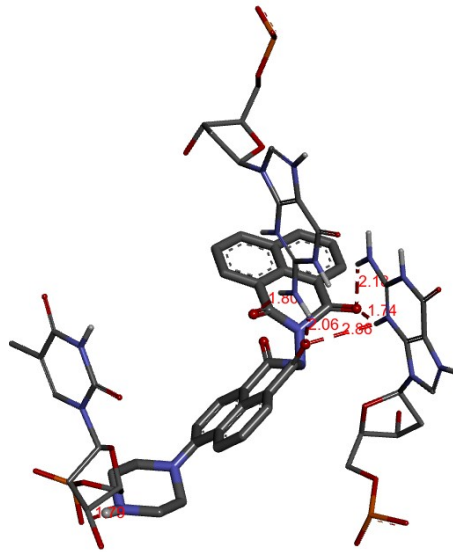


Conventional Hydrogen Bond



Pi-Sigma

5g

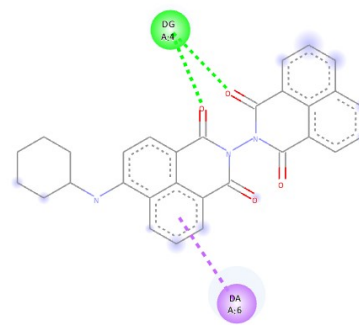
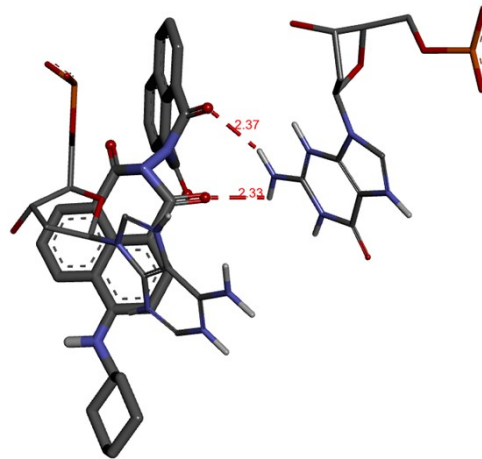


Interactions



Conventional Hydrogen Bond

5h



Interactions

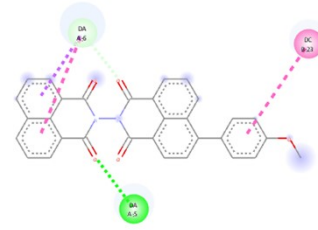
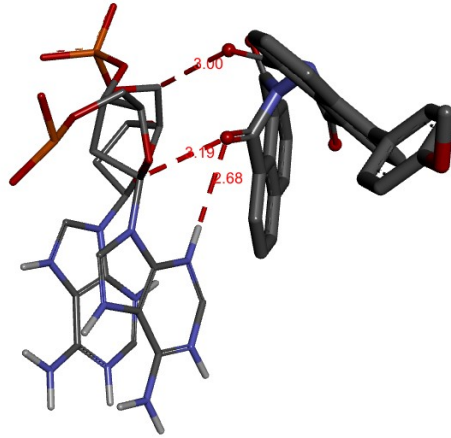


Conventional Hydrogen Bond



Pi-Sigma

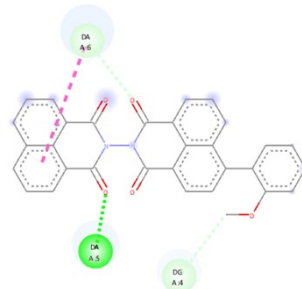
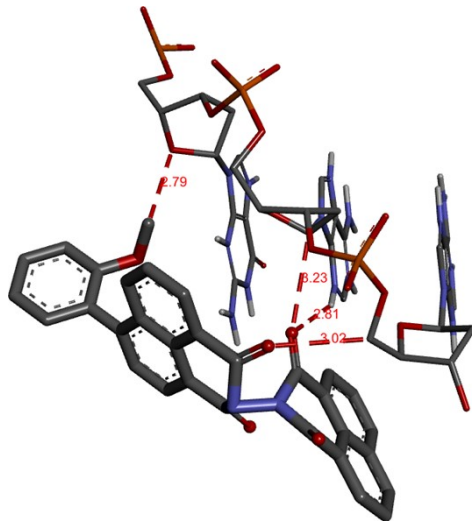
5i



Interactions

- | | | | |
|---|----------------------------|---|----------------|
|  | Conventional Hydrogen Bond |  | PI-PI Stacked |
|  | Carbon Hydrogen Bond |  | PI-PI T-shaped |
|  | PI-Sigma | | |

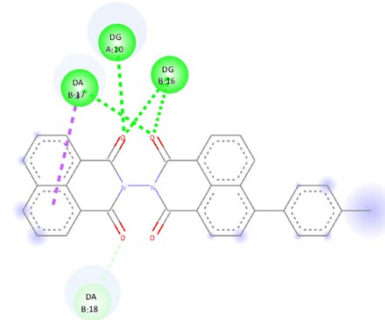
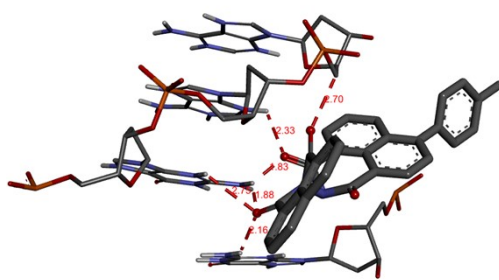
5j



Interactions

- | | | | |
|---|----------------------------|---|---------------|
|  | Conventional Hydrogen Bond |  | PI-PI Stacked |
|  | Carbon Hydrogen Bond |  | PI-Alkyl |

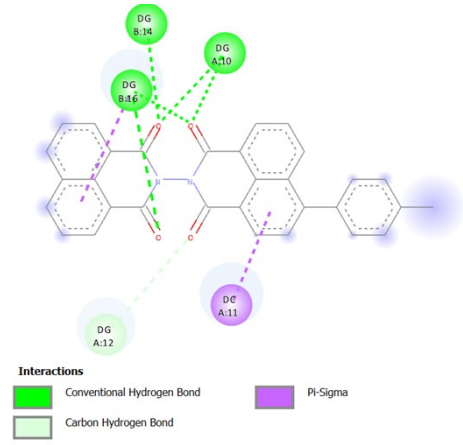
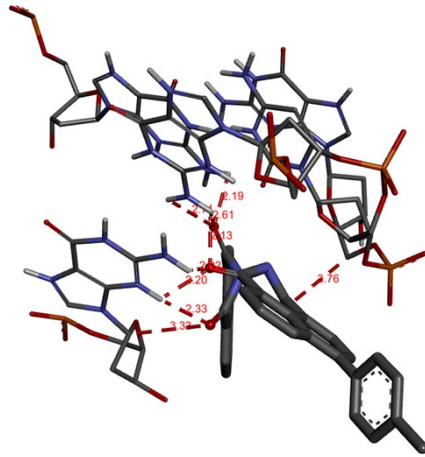
5k



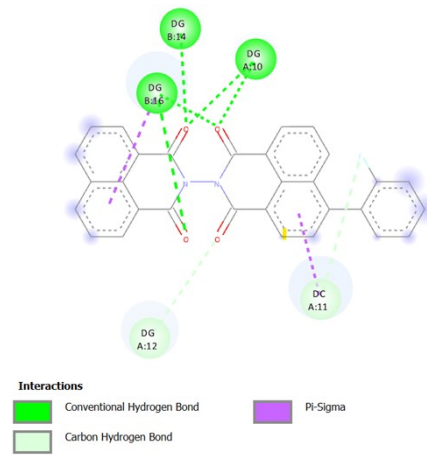
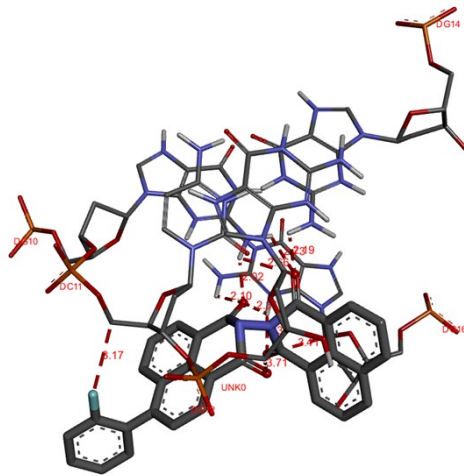
Interactions

- | | | | |
|---|----------------------------|---|----------|
|  | Conventional Hydrogen Bond |  | PI-Sigma |
|  | Carbon Hydrogen Bond | | |

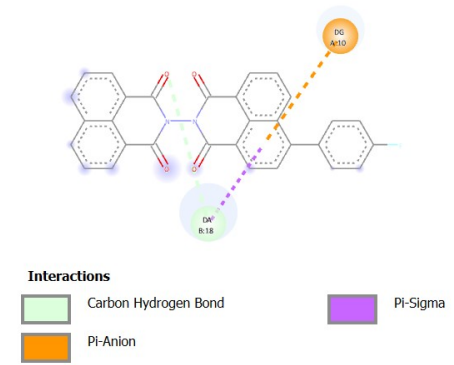
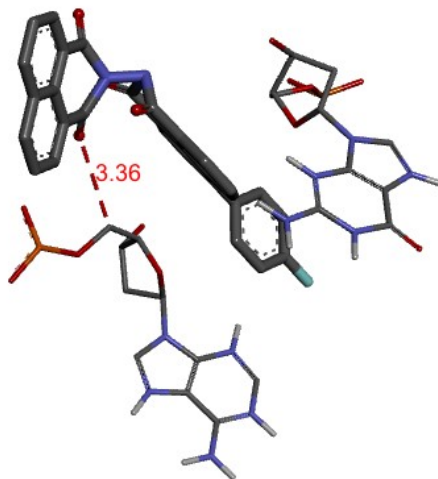
5l



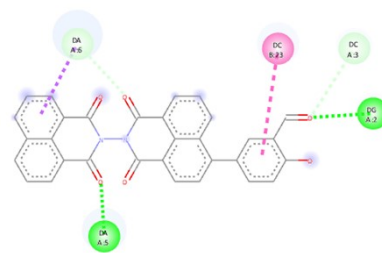
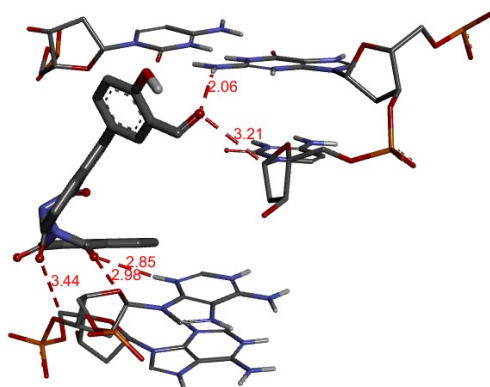
5m



5n



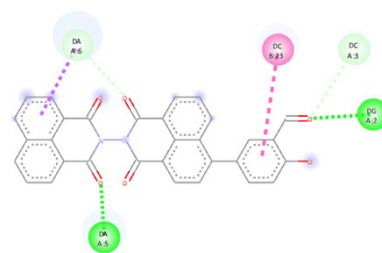
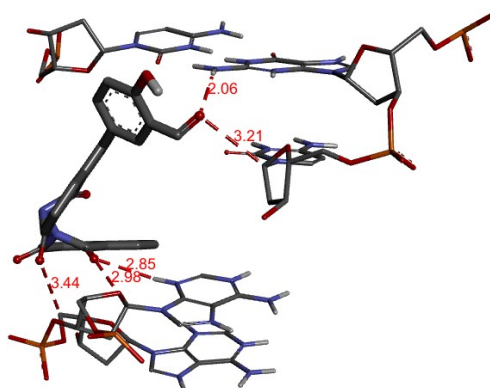
5o



Interactions



5p



Interactions



Table S11. The docking results based on the binding free energies (kcal/mol) of compounds **5d** and **5o** docked into 1BNA from the co-crystallized ligand

Mode	5d	5o
1	-10.56	-10.98
2	-10.03	-9.26
3	-9.31	-9.26
4	-9.28	-9.24
5	-8.24	-9.03
6	-8.09	-8.86
7	-8.05	-8.82
8	-7.79	-8.81
9	-6.86	-8.81

Table S12. The docking results based on the binding free energies (kcal/mol) of different compounds (**5a – 5h**) docked into 1BNA

Mode	5a	5b	5c	5e	5f	5g	5h
1	-9.69	-9.61	-9.98	-9.42	-10.05	-9.26	-10.38
2	-9.61	-9.59	-9.76	-9.25	-10.04	-9.23	-9.49
3	-8.03	-7.71	-8.85	-8.83	-9.99	-9.13	-9.26
4	-8.03	-7.69	-8.58	-8.82	-9.79	-9.1	-8.76
5	-8.02	-7.65	-8.53	-8.8	-9.7	-9.09	-8.68
6	-8.02	-7.55	-8.52	-8.79	-9.56	-9.08	-8.56
7	-7.98	-7.38	-8.5	-8.74	-9.21	-9	-8.53
8	-7.81	-7.36	-8.49	-7.88	-8.94	-8.1	-8.49
9	-7.78	-7.33	-8.45	-7.78	-8.58	-7.45	-8.41
10	-7.76	-7.28	-8.44	-7.05	-7.34	-7.07	-8.71

Table S13. The docking results based on the binding free energies (kcal/mol) of different compounds (**5i -5p**) docked into 1BNA

Mode	5i	5j	5k	5l	5m	5n	5p
1	-8.61	-9.16	-9.59	-8.76	-9.63	-9.2	-8.74
2	-8.5	-9.15	-9.22	-8.75	-9.21	-9.17	-8.73
3	-8.5	-9.13	-9.2	-8.72	-9.08	-9.14	-8.65
4	-8.49	-8.99	-9.13	-8.72	-9.08	-9.14	-8.71
5	-8.49	-8.94	-8.99	-8.71	-9.07	-9.13	-8.69
6	-8.4	-8.74	-8.91	-8.71	-9.07	-9.13	-8.67
7	-7.96	-8.71	-8.91	-8.52	-9.05	-9.12	-8.67
8	-7.94	-8.49	-8.9	-8.31	-9.04	-9.1	-8.66
9	-7.93	-8.49	-8.82	-8.31	-9	-9.07	-8.65
10	-7.84	-7.87	-8.48	-8.25	-8.83	-8.83	-8.64

HSA binding studies

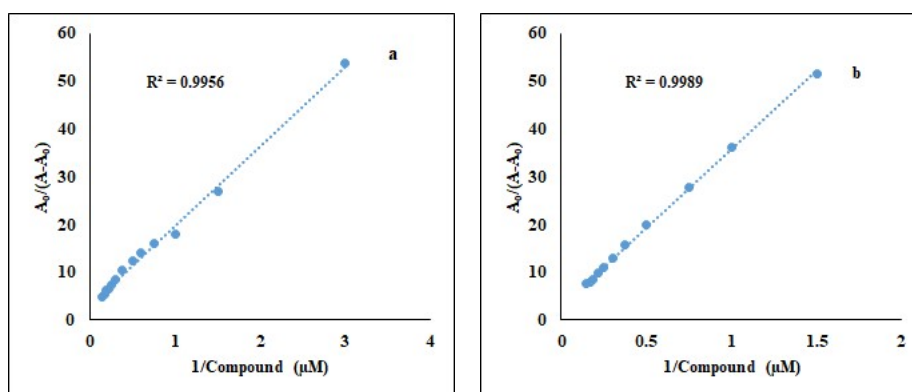


Figure S36. Benesi-Hildebrand plots $\{A_0/(A-A_0) \text{ vs. } 1/[\text{compound}]\}$ of absorption spectra of HSA in the absence and presence of (a) compound **5d** and (b) compound **5o** at 298 K

Table S14. Binding parameters for compound **5d** and **5o** at 298 K

Compound	K_{sv} (10^5 M^{-1})	K_q ($10^{13} \text{ M}^{-1} \text{ S}^{-1}$)	aR	K_b (10^4 M^{-1})	n	aR
5d	0.6	0.6	0.9954	2.4	0.95	0.9928
5o	1.6	1.6	0.9934	18.5	1.0	0.9949

aR is the correlation coefficient

Table S15: Thermodynamic parameters of HSA binding with compounds **5d** and **5o**

T (K)	ΔG , kcal M^{-1} (5d)	ΔG , kcal M^{-1} (5o)
298	-5.96	-7.18

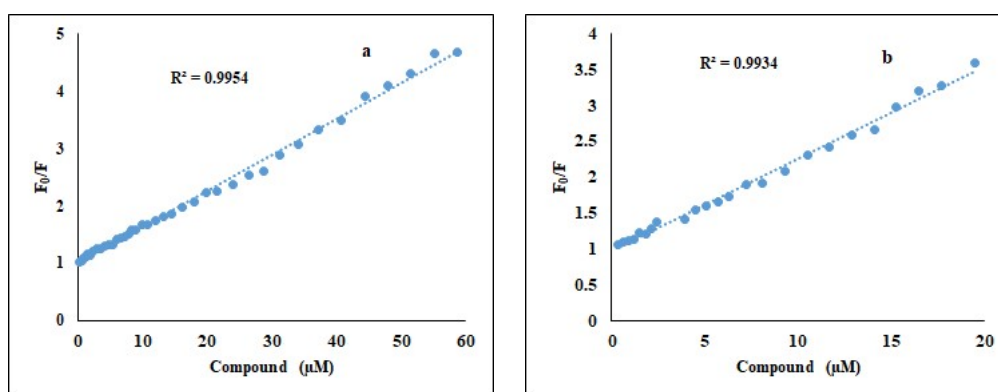


Figure S37. Stern-Volmer plots $\{F_0/F \text{ vs. } [\text{compound}]\}$ of emission spectra of HSA in the absence and presence of (a) compound **5d** and (b) compound **5o** at 298 K

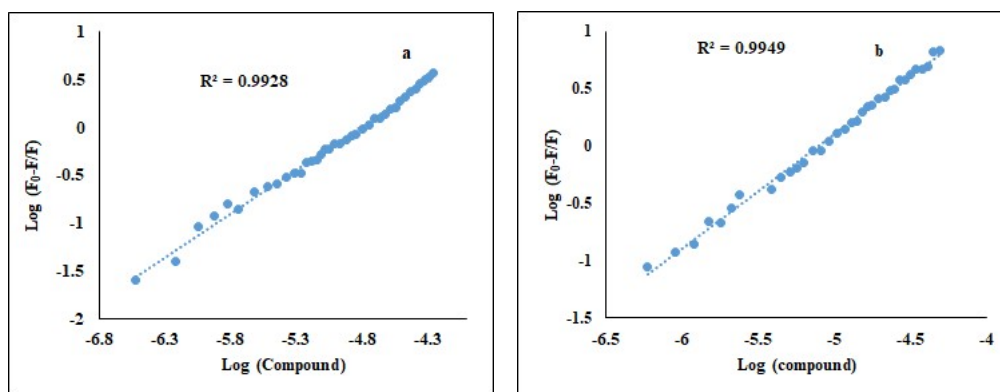


Figure S38. Modified Stern-Volmer plots { $\log [(F_0-F)/F]$ vs. $\log [\text{compound}]$ } of emission spectra of HSA in the absence and presence of (a) compound **5d** and (b) compound **5o** at 298K

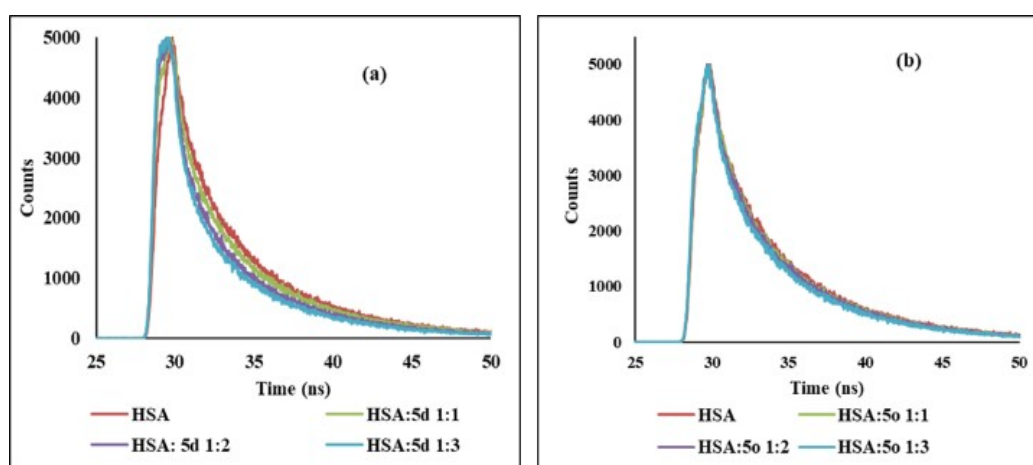


Figure S39: Time decay profile of HSA on progressive addition of compounds (a) **5d** and (b) **5o** in phosphate buffer (pH 7.4).

Table S16. Lifetime fluorescence decay of HSA on interaction with **5d** and **5o**

System	Conc.	τ_1 [ns]	τ_2 [ns]	τ_3 [ns]	α_1	α_2	α_3	T_{av}	χ^2
HSA		2.8	6.64	0.57	0.56	0.1	0.09	3.12	1.16
HSA-5d	01:01	2.44	6.35	0.45	0.34	0.09	0.04	2.23	1.17
	01:02	2.05	6.1	0.35	0.29	0.08	0.47	1.63	1.18
	01:03	2.01	6.06	0.32	1.36	0.27	0.09	1.36	1.20
HSA-5o	01:01	2.94	6.63	0.64	0.67	0.12	0.09	3.1	1.15
	01:02	3.11	6.7	0.66	0.71	0.13	0.4	3.06	1.18
	01:03	2.93	6.48	0.64	0.68	0.14	0.08	2.85	1.2

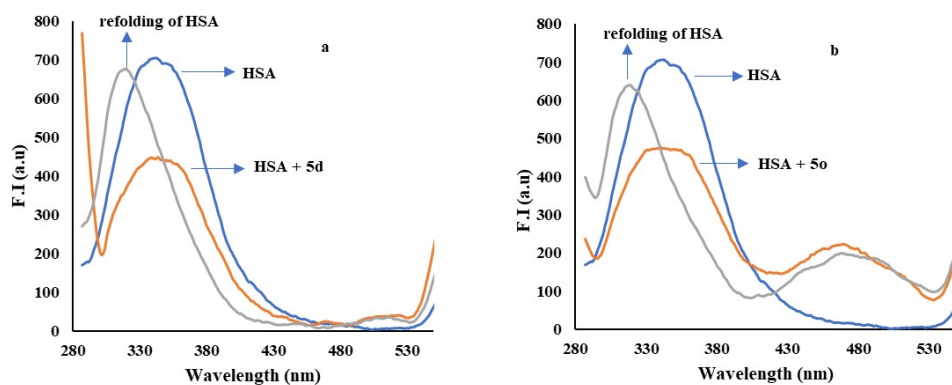
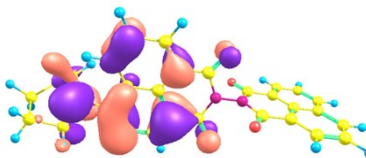
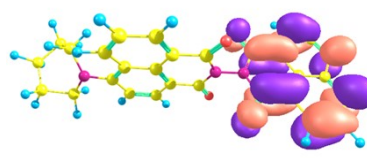
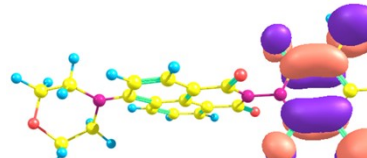
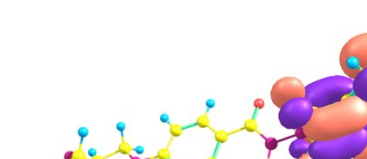
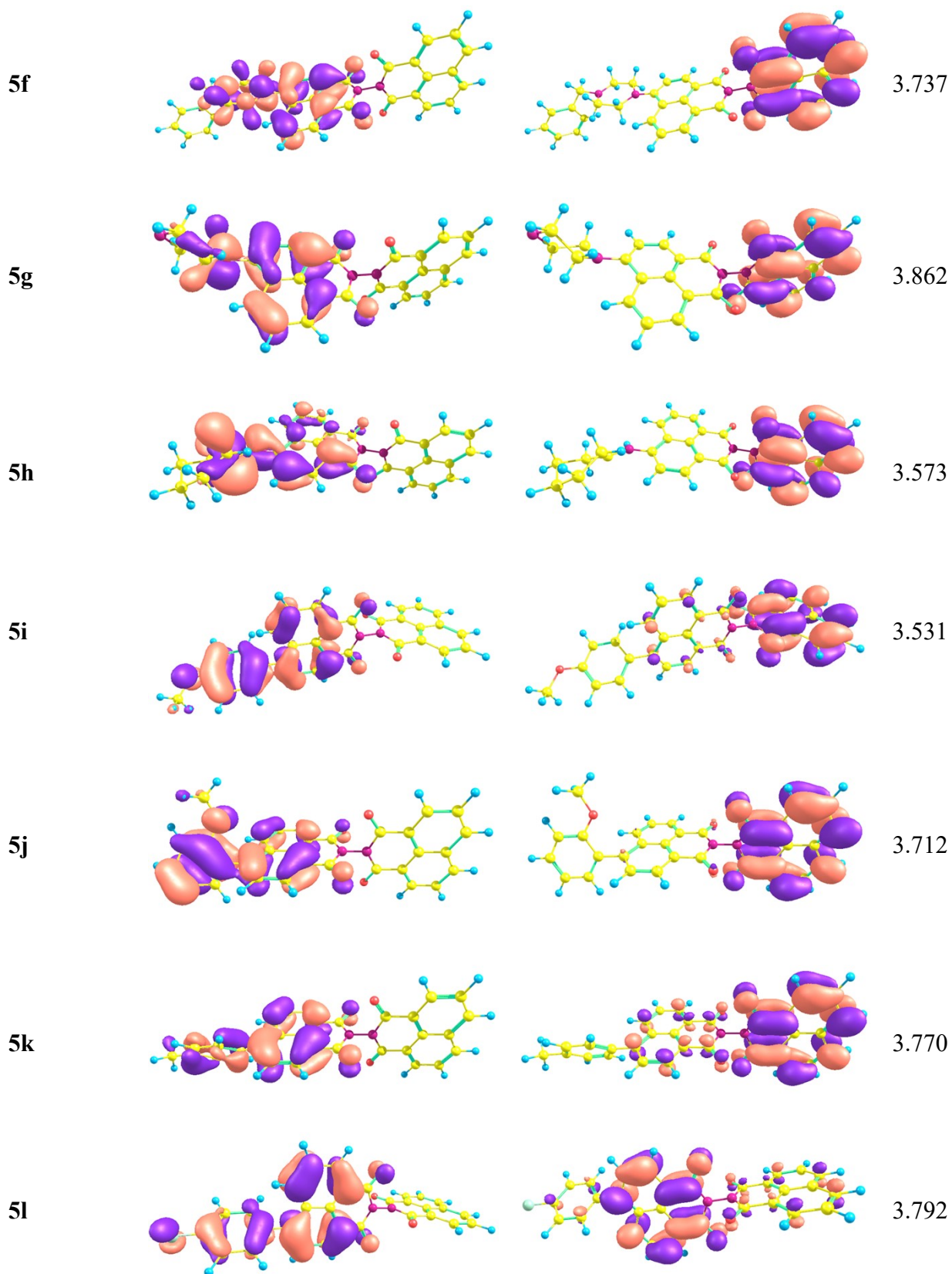
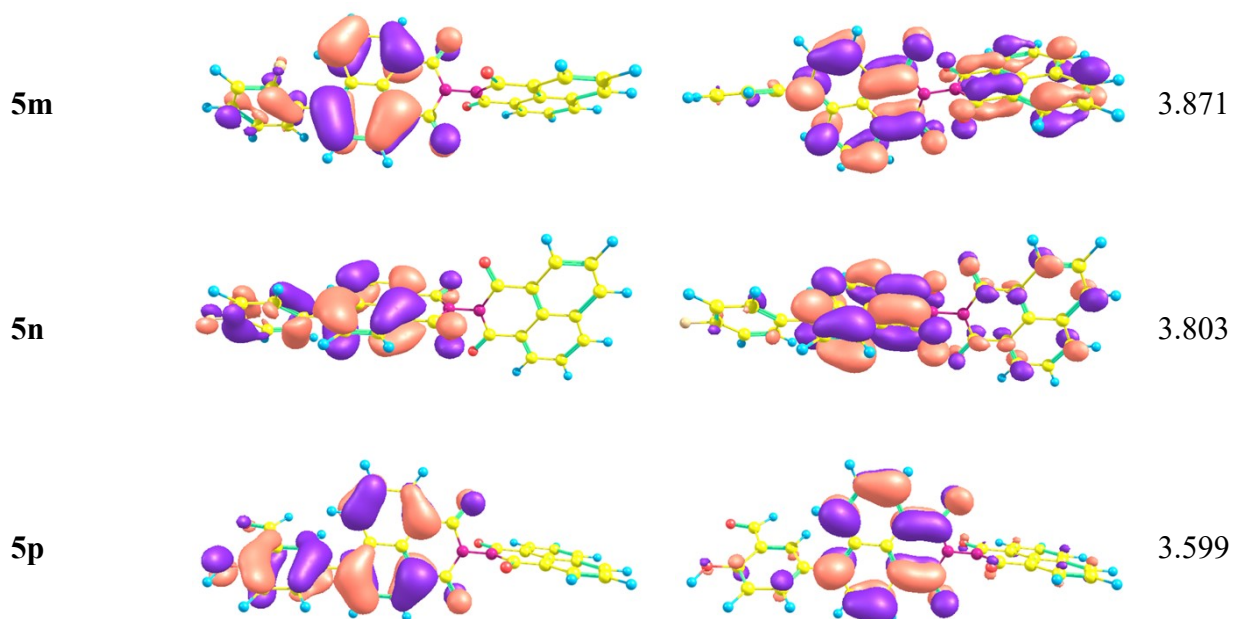


Figure S40: Fluorescence spectra of bare HSA (blue) in the presence of compounds (a) **5d** (orange) and (b) **5o** (red) and in the presence of SDS (grey).

Table S17: Atomic orbitals HOMO-LUMO composition of compounds (**5a – 5p**)

Compound	HOMO (eV)	LUMO (eV)	ΔE (eV)
5a			3.642
5b			3.462
5c			3.820
5e			3.576





Sample preparation

The stock solutions of HSA (10^{-3} M) were prepared in water, the compounds **5d** and **5o** were prepared in DMSO, and all the studies were conducted in phosphate buffer.

UV-Vis absorption spectroscopy

The absorption spectra of free HSA, **5d**-HSA, **5o**-HSA systems have been recorded in phosphate buffer (*pH* 7.4) from 200 to 800 nm wavelength range at 298 K. The HSA interaction study was performed by taking HSA ($10\ \mu\text{M}$) and increasing the concentration of compounds **5d** (0 - $10\ \mu\text{M}$) and **5o** (0 - $8\ \mu\text{M}$). The binding constants were determined using the following Benesi-Hildebrand equation (eq.-3)-

$$\frac{A_0}{(A - A_0)} = \frac{\varepsilon_f}{(\varepsilon_b - \varepsilon_f)} + \frac{\varepsilon_f}{(\varepsilon_b - \varepsilon_f) K_b [\text{Analyte}]}$$

----- (3)

A_0 denotes the absorbance of free HSA, whereas A denotes the absorbance of bound form of HSA with derivatives **5d** and **5o**. In this equation, ε_f and ε_b denote the molar extinction coefficients of HSA in free and fully bound form, respectively. The values of binding constant (K_b) was estimated using the ratio of intercept-to-slope of the $A_0/(A - A_0)$ and $1/[\text{compound}]$ plot.

Fluorescence emission spectroscopy

The emission spectra of HSA have been recorded in phosphate buffer (*pH* 7.4) from 200 to 800 nm wavelength range. The HSA interaction study was performed by taking HSA ($10\ \mu\text{M}$) and increasing concentration of compounds **5d** (0 - $60\ \mu\text{M}$) and **5o** (0 - $20\ \mu\text{M}$) at 298 K. The binding

constant was determined using following Stern-Volmer equation (eq.-4) and modified Stern-Volmer equation (eq.-5)-

$$\frac{F_0}{F} = 1 + K_{sv} [\text{Analyte}] = 1 + K_q \tau_0 [\text{Analyte}] \text{----- (4)}$$

$$\log \frac{F_0 - F}{F} = \log K_b + n \log [\text{Analyte}] \text{----- (5)}$$

F₀ denotes the fluorescence intensity of free HSA (HSA study) whereas F denotes the bound form of HSA with derivative **5d** and **5o** (HSA study). The values of the quenching constant (K_{sv}) were estimated using the ratio of the slope-to-intercept of F₀/F and [compound] plot. To determine the quenching rate constant (K_q), average fluorescence lifetime (τ₀) value of 10⁻⁸ s was used.³ The intercept and slope of log[(F₀-F)/F and log [analyte] plots were used to calculate the values of the binding constant (K_b) and the number of the binding sites (n), respectively. The Van't Hoff equation (eq.-6) and equations-5 were used to calculate the thermodynamic parameters-

$$\log K_b = -\frac{\Delta H}{2.303RT} + \frac{\Delta S}{2.303R} \text{----- (4)}$$

$$\Delta G = -2.303RT \log K_c$$

Where R denotes the gas constant and T denotes the temperature (K). ΔG is the Gibb's free energy and K_c is binding constant.

Competitive displacement assay

Ethidium bromide dye displacement assay was recorded by using a fixed amount of ethidium bromide and ct-DNA (3 μM: 30 μM) with increasing concentrations of compound **5d** (0-30 μM) and **5o** (0-40 μM). Emission spectra were recorded using 520 nm as excitation wavelength.

Docking Simulation

Molecular docking of all the compounds with DNA (PdB: 1BNA) was carried out using the AutoDock package (vina). In the preparation of target (DNA), water molecules were deleted, whereas all polar hydrogens were added to the target, then calculated gasteiger charges. The 3D structure of all the compounds were optimized using the Gaussian 09W program and the resulted from the file was saved as pdb format. The ADT package was used to modify the partial charges of the ligand and the resulted file was saved as pdbqt format. A grid having spacing 0.375 Å and pointing 44 Å, 78 Å, 106 Å in x, y, and z directions, respectively were used.

References

1. Sun, H.; Ansari, M. F.; Battini, N.; Bheemanaboina, R. R. Y.; Zhou, C. H. Novel Potential Artificial MRSA DNA Intercalators: Synthesis and Biological Evaluation of Berberine-Derived Thiazolidinediones. *Org. Chem. Front.* 2019, 6 (3), 319–334.
2. Anticancer activity at NCI https://dtp.cancer.gov/discovery_development/nci-60/methodology.htm (accessed in April 2019).
3. J.R.; Lakowicz, G.; Weber, Quenching of Protein Fluorescence by Oxygen. Detection of Structural Fluctuations in Proteins on the Nanosecond Time Scale. *Biochem.* **1973**, 12, 4171–4179.